NAVAL FACILITIES ENGINEERING SERVICE CENTER
Port Hueneme, California 93043-4370

Technical Memorandum
TM-2248-AMP

HYDRODYNAMIC LOAD RESPONSE OF A MODULAR PLATFORM DUE TO WAVES -- A PARAMETRIC STUDY

by

Reuybin (Ray) Chiou, Ph. D., PE

March 1997

Executive Summary

In support of the U.S. Navy's Logistics Over the Shore (LOTS) operation in high sea states, the Naval Facilities Engineering Service Center (NFESC) has proposed to develop an advanced modular causeway lighterage/platform system that promises significant advances in the Navy's LOTS operation. NFESC selected an advanced lighter design that was based on a building block concept through an initial R & D effort. This design, the Amphibious Cargo Beaching (ACB) Lighter, uses a 40-ft long by 24-ft wide and 8-ft deep module that would be easy to transport and assemble on site. The modules can be assembled into a larger platform of desired size by using inter-module connectors in both longitudinal and transverse directions. The modularity of this system provides the ability for the users to assemble platforms of various sizes and configurations to meet their changing needs at the forward logistics site.

The operation and survival of the system in higher sea states depends on the adequate design of the connectors. In support of the connector design, the objective of this study is to determine design loads applied to the connectors by the wave forces. The approach is to perform a parametric study by using a diffraction theory-based program to determine the hydrodynamic response of the platform in different environments specified by sea state and various wave directions. The platform dimensions used in the parametric study range from 80 feet to 200 ft long (i.e., 2 to 5 modules) and from 24 ft to 72 ft wide (i.e., 1 to 3 modules). This report summarizes the results of this parametric study on connector/section loads through the hydrodynamic and dynamic analysis of platforms composed of modules.

Table of Contents

List of Figures

Page

List of Figures (cont.)

Page

List of Tables

Page

1.0 INTRODUCTION

In support of the U.S. Navy's Logistics Over the Shore (LOTS) operation in high sea states, the Naval Facilities Engineering Service Center (NFESC) has proposed the development of an advanced modular causeway lighterage/platform system that promises significant advances in the Navy's LOTS operation. This revolutionary lighter, the Amphibious Cargo Beaching (ACB) Lighter, will allow operation in higher sea states than the current barrier of sea state two. In addition, the system will be readily deployable from available lift assets. The modularity of this system provides the ability for the users to assemble platforms of various sizes and configurations to meet their changing needs at the forward logistics site.

After an initial R & D effort to resolve the deficiencies of existing causeway systems, NFESC selected an advanced lighter design that was based on a building block concept. The design uses a 40-ft long by 24-ft wide and 8-ft deep module that would be easy to transport and assemble on site. The modules can be assembled into a larger platform of desired size by using inter-module connectors in both longitudinal and transverse directions. For example, three modules in the longitudinal direction and two modules in the transverse direction will be required to form a 120 ft-by-48 ft-by-8 ft platform.

The objective of this study is to determine design loads applied to the connectors by the wave forces as well as to investigate the feasibility of large platform sizes. The approach is to perform a parametric study by running the computer program MORA [Ref. 1] with different environmental parameters specified by sea state and various wave directions. The platform dimensions used in the parametric study range from 80 feet to 200 ft long (i.e., 2 to 5 modules) and from 24 ft to 72 ft wide (i.e., 1 to 3 modules). The term "m by n" platform, hereafter, will represent a platform composed of m modules in the longitudinal direction and n modules in the transverse direction. For example, a 3 x 2 platform which is composed of three modules in the longitudinal direction and two modules in the transverse direction is illustrated in Figure 1.1. The rectangular coordinate system used to describe the loads is also shown in this figure; its origin is located at the centroid of the platform with the X-axis lying along the long dimension of the platform, the Y-axis directed upward, and the Z-axis directed in the beamwise direction. Figure 1.2 shows the definition of internal loads and wave direction.

In order to determine the loads which must be resisted by the connectors to form a rigid platform, a number of structural analyses using the free body isolated from the platform must be conducted. The selection of the free body is primarily determined by the location of connectors along the longitudinal (at X = constant) and transverse (at Z = constant) directions. For example, an imaginary cut through a 2 x 1 platform must be used through a vertical plane at X = 0 ft where the connectors are present in order to isolate a free body equaling to one half of the platform. However, in some cases the free body cuts were used at the location where the maximum section loads were anticipated. These section loads can be used for the module design and should not be confused with the connector loads. For example, the imaginary cuts at X = 0 ft and Z = 0 ft for a 5x3 platform will provide the section loads rather than the connector loads. The statistical values of all six components of the internal loads including three components of forces and three components of bending moments will be available from each free body analysis.

This report summarizes the results of this parametric study on connector/section loads through the hydrodynamic and dynamic analysis of platforms assembled from modules.

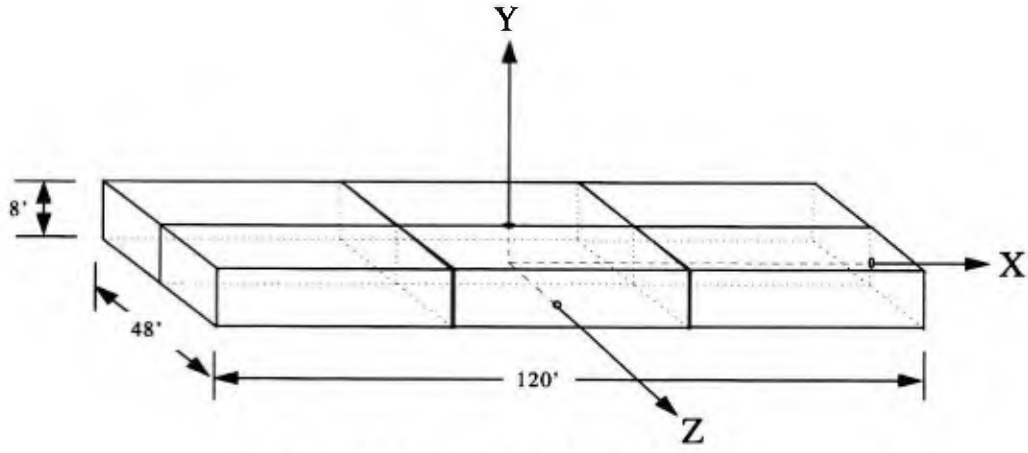

Figure 1.1 Illustration of a 3 x 2 Platform

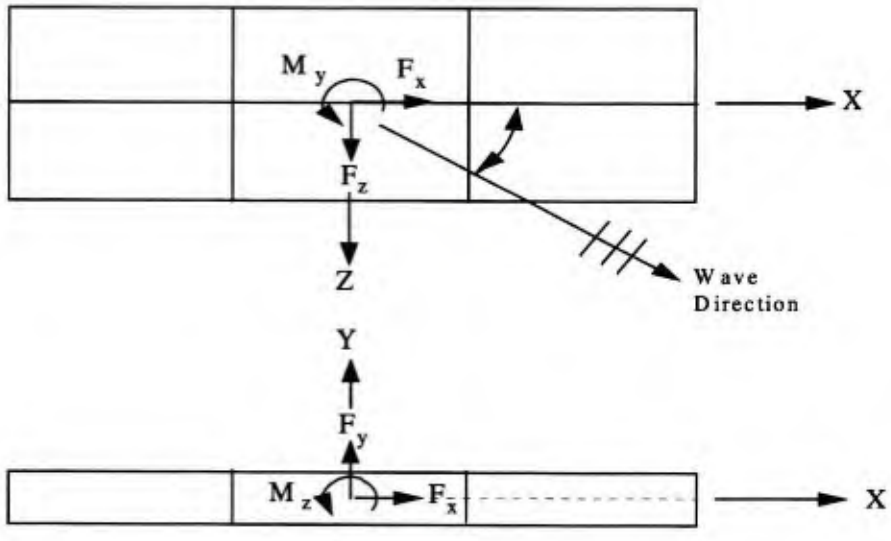

Figure 1.2 Definition of Internal Loads and Wave Direction

2.0 CONNECTOR / SECTION LOADS DUE TO WAVE EXCITATION

2.1 Methodology

The calculation of connector/section loads due to wave forces is executed based on the assumption that a rigid platform can be assembled by joining individual modules through the use of connectors in both longitudinal and transverse directions. This connector load calculation is one of many key pieces of information required for connector design. In order to calculate the connector/section load, it is essential to first perform a hydrodynamic analysis of the assembled platform in waves based on the three-dimensional diffraction theory such that basic frequency-dependent hydrodynamic coefficients (both added mass and radiation damping coefficients), excitation loads, and mean-drift loads will be available for structural analysis in the next phase of analysis. In the next step of the analysis, the response amplitude operator (RAO) for the load components at the cross section associated with the free body must be computed. This RAO information for the load components is then used in conjunction with the wave spectrum to obtain the connector/section load response.

2.2 Hydrodynamic Analysis

The hydrodynamic analysis of the platform is performed using computer program MORA which was developed by C.J. Garrison and Associates [Ref. 1]. The program is based on a three-dimensional diffraction theory. It can compute the hydrodynamic coefficients, excitation load coefficients, and mean drift-loads for a large-displacement body based on the boundary element method. The program is developed by discretizing the immersed surface of the body into quadrilateral or triangular panels such that distributed sources of uniform strength can be placed on the panels and the strengths be adjusted in order to satisfy the no-flow boundary condition on the immersed surface. Intermediate results of the program include both velocity and pressure distributions over the immersed surface. The pressure distribution is then integrated over the immersed surface to obtain the hydrodynamic coefficients. Refer to the MORA User's Guide for a detailed description of its capability.

The use of MORA for hydrodynamic analysis as described above requires the immersed surface of the platform to be discretized into quadrilateral or triangular panels. The subdivision of the immersed surface must be fine enough to warrant a convergence of a numerical solution, but should not be too fine such that excessive computational time is required. The guideline for selecting an appropriate panel size is to plot hydrodynamic coefficients versus wave excitation frequencies so that curves representing hydrodynamic coefficients can be visually inspected. If the curves across the frequency range of interest are not very smooth, it is recommended that the program be re-run with finer panels in order to obtain a set of more accurate hydrodynamic coefficients.

The typical panel size used in the analysis is approximately 4 ft by 4 ft. This will subdivide a 2x1 platform into 160 panels and a 5x3 platform into 1,000 panels. The 2x1 platform measured 80 ft-by-24 ft-by-8 ft is the smallest structure studied while the 5x3 platform measured 200 ft-by-72 ft-by-8 ft is the largest. The draft of the immersed surface for all the cases reported here is 3.49 ft. This value is based on the assumption of 30 long tons of self-weight and 70 short tons of cargo load for each module. The raked end module for the assembled platform is assumed to have a 45 degrees slope. No surface or subsurface current is considered in performing hydrodynamic analyses for this study. The platform is considered to be free floating without any moorings. Figures 2.1 and 2.2 show the subdivided immersed surface for a 2x1 and a 5x3 platform respectively.

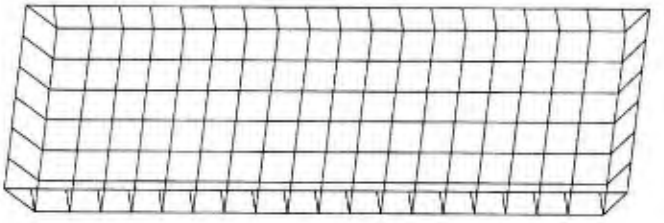

Figure 2.1 Subdivided Immersed Surface for a 2 x1 Platform

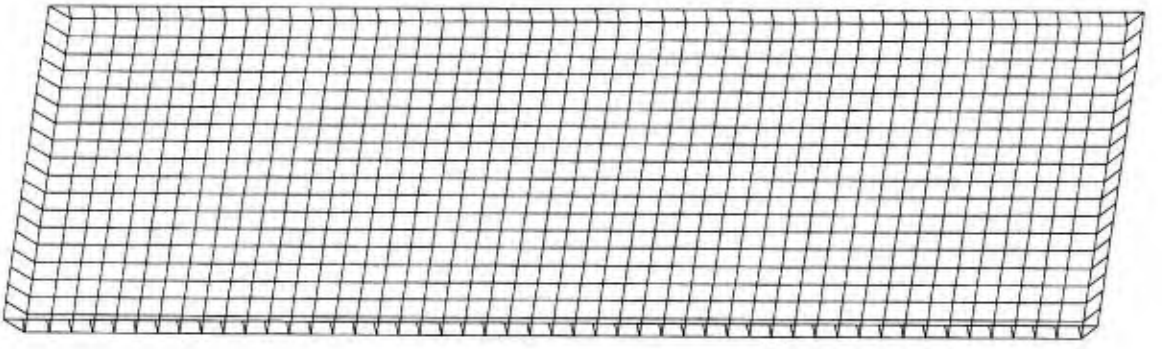

Figure 2.2 Subdivided Immersed Surface for a 5 x3 Platform

Typical hydrodynamic coefficients are displayed in Figures 2.3 through 2.6 where the added mass coefficients are denoted by M_{ij} and damping coefficients by N_{ij}. The subscripts i=1,2,3 are associated with the surge, heave, and sway motions while subscripts j =4,5,6 are associated with the roll, yaw, and pitch. For example, M_{22} represents the added mass for heave motion and M_{66} is the added mass for pitch motion. Similarly, N_{22} represents the damping coefficient for heave motion and N_{66} is the damping coefficient for pitch motion.

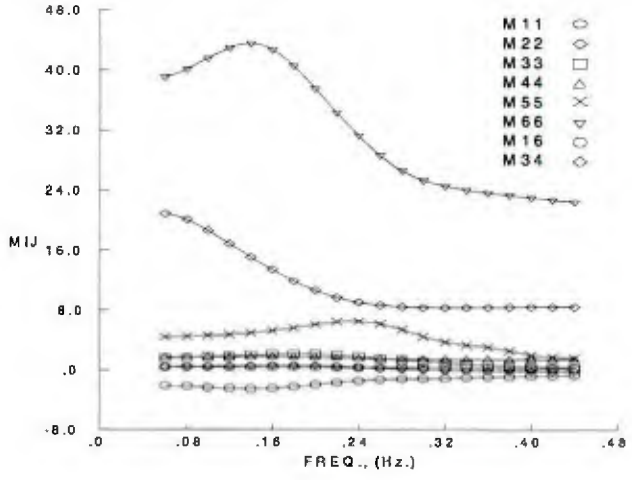

Figure 2.3 Added Mass Coefficients (2x1 Platform)

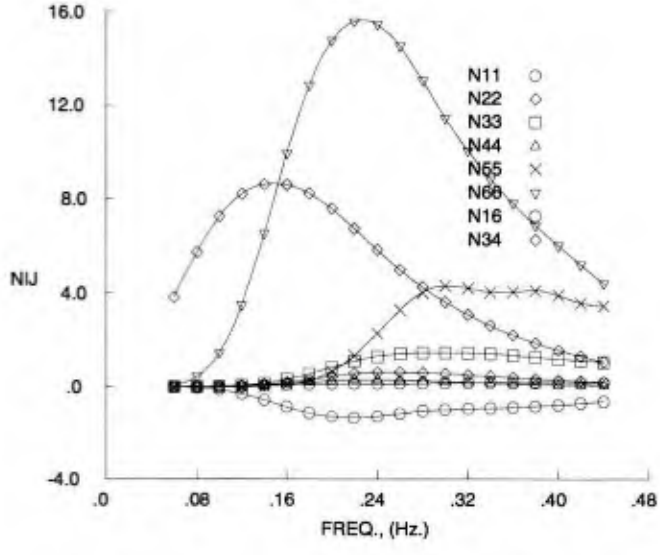

Figure 2.4 Damping Coefficients (2x1 Platform)

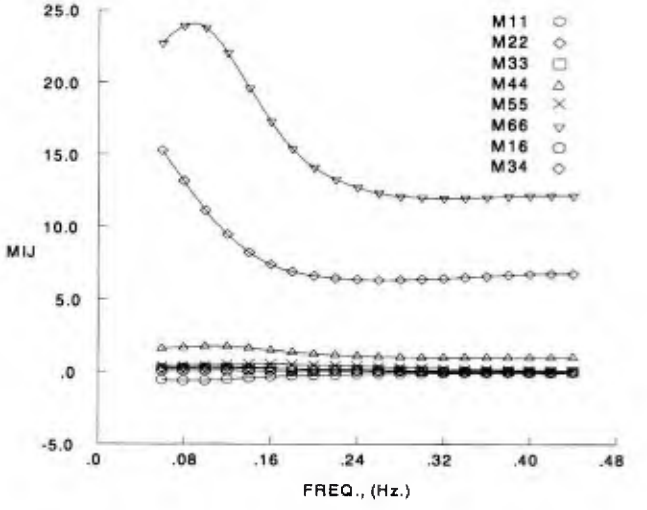

Figure 2.5 Added Mass Coefficients (5x3 Platform)

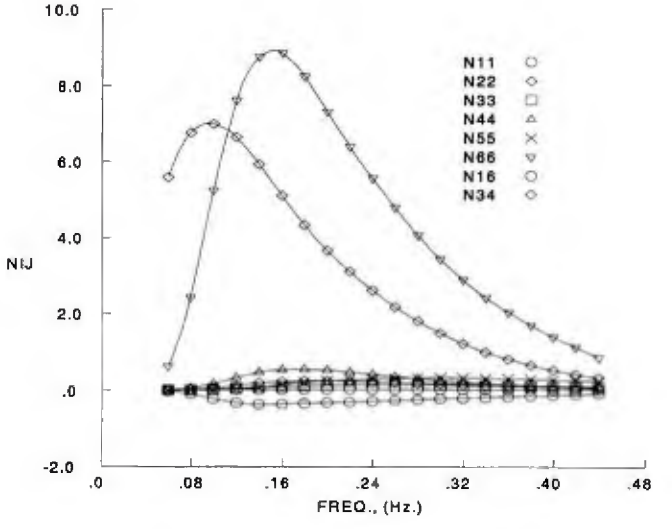

Figure 2.6 Damping Coefficients (5x3 Platform)

2.3 Wave Spectra

Two wave spectra are used in conducting this parametric study: an operational spectrum represented by sea state 3 (SS3) and a survival sea state 5 (SS5). These spectra are characterized by the ISSC (International Ship Structures Congress) spectra. The significant wave height, H_s, and the peak frequency, f_o, are 3.3 ft and 0.18 Hz for SS3, and 10 ft and 0.11 Hz for SS5. These two spectra are plotted and shown in Figures 2.7 and 2.8 below.

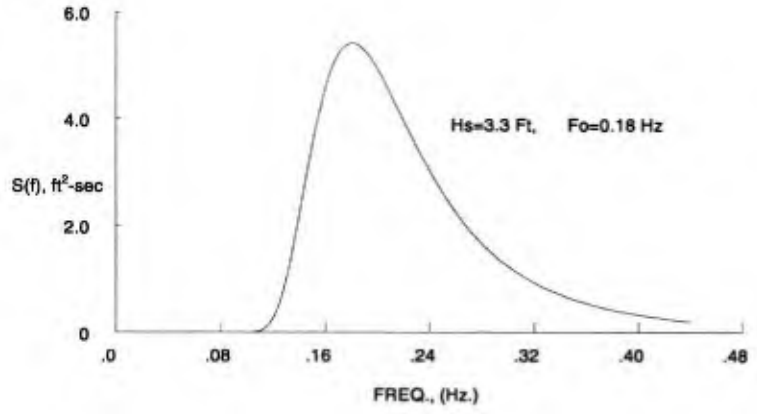

Figure 2.7 ISSC Wave Spectrum (SS3)

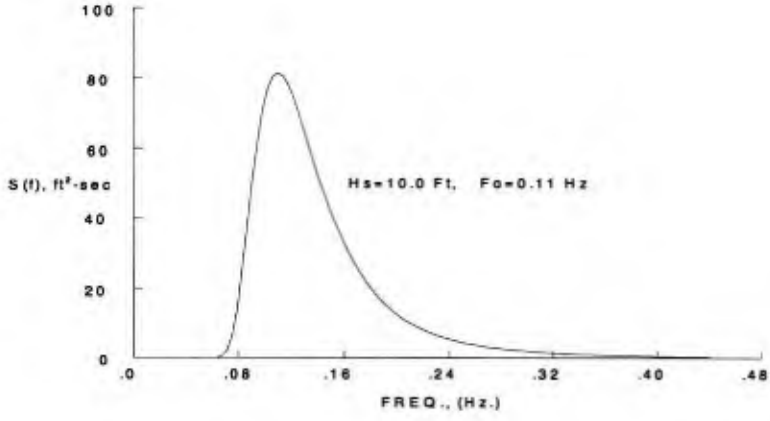

Figure 2.8 ISSC Wave Spectrum (SS5)

2.4 Mass Properties

In order to compute the platform motion and connector/section loads, the mass properties of the platform are required. Table 2.1 shows the mass and mass moment of inertia of the entire structure for the 2x1 and 5x3 platforms. Table 2.2 shows the mass and mass moment of inertia of the free body isolated by the imaginary cuts at X=0 ft or Z=0 ft for the 2x1 and 5x3 platforms. The mass properties are calculated by assuming each module weighs 30 long tons and carries 70 tons of cargo. Furthermore, the mass of the platform is assumed to be uniformly distributed over the surface of the rectangular box-like shell structure. The mass of the free body corresponds to the part of platform located on the positive X-axis or Z-axis side of the cut. All of the mass moments of inertia I_{xx}, I_{yy}, and I_{zz}, are calculated with respect to the body coordinates located at the centroid of the entire platform. Other mass moments of inertia, I_{xy}, I_{yz}, and I_{xz}, are equal to zero because of symmetry.

Table 2.1 Mass Properties of the Entire Platform

Platform	Mass (slugs)	I_{xx} (slug-ft^2)	I_{yy} (slug-ft^2)	I_{zz} (slug-ft^2)
2 x 1	12,870	1.07×10^6	8.73×10^6	7.99×10^6
5 x 3	96,522	5.12×10^7	3.94×10^8	3.46×10^8

Table 2.2 Mass Properties of the Free Body
(Imaginary Cuts at X=0 ft or Z=0 ft)

Platform	Mass (slugs)	I_{xx} (slug-ft^2)	I_{yy} (slug-ft^2)	I_{zz} (slug-ft^2)
2 x 1	6,435	5.35×10^5	4.36×10^6	3.99×10^6
5 x 3	48,261	2.56×10^7	1.97×10^8	1.73×10^8

2.5 Connector / Section Loads

There are three components of force and three components of bending moment associated with each degree of freedom of motion computed for each free body isolated by the imaginary cuts either along the X-axis or Z-axis. These connector/section loads are computed for both the operational environment (SS3) and survival environment (SS5). In all cases, the connector/section loads are computed for different wave directions (as defined in Figure 1.2) ranging form 0 degrees to 90 degrees with an increment of 15 degrees. According to the definition of wave direction, 0-degree waves represent head seas while 90-degree waves represent beam seas.

The internal (i.e., connector or section) loads computed by MORA are given in both static loads and significant loads. The static loads are computed by taking into account only the weights and buoyancy

while the significant loads include the wave loads. From the structural design point of view, the maximum connector/section loads are of primary concern. Therefore, the following figures show only the maximum connector/section loads rather than the significant loads. Based on a Rayleigh distribution, the maximum connector/section loads can be obtained by multiplying the significant loads by a factor that depends on the cycles of the wave excitations. The most-used multiplier of 1.86 corresponds to 1000 cycles of wave excitations. In this study, the maximum connector/section loads are calculated by adding two times the significant load to the static load.

Figures 2.9 and 2.10 show the maximum section loads at X=0 ft for the 5x3 platform in operational seas. These two figures are typical for all the cases studied. Because of the shape of the platform with a shallow draft of 3.49 ft, it is obvious that the section loads, F_x and F_z are relatively smaller than F_y. This is due to the fact that the submerged area of the platform in the X direction or Z direction is quite small compared to the submerged area in the Y direction. Thus, the force component, F_y is the only section loads component among force components shown in the subsequent section. Based on this same reasoning, the bending moment component, M_x, is relatively small. The bending moment component, M_y, is at its peak for the beam seas environment and has a comparable magnitude to bending moment M_z. This is due to the fact that the platform responds to the beam seas with significant roll motion (approximately 3.2 degrees). This in turn causes increases in the pressure force component acting in the direction of Z-axis and, subsequently, a significant amount of bending moment about the Y-axis. However, this bending moment can be easily resisted based on the large section modulus available compared to the small section modulus available to resist the bending moment M_z. Consequently, the subsequent section only shows the bending moment component, M_z.

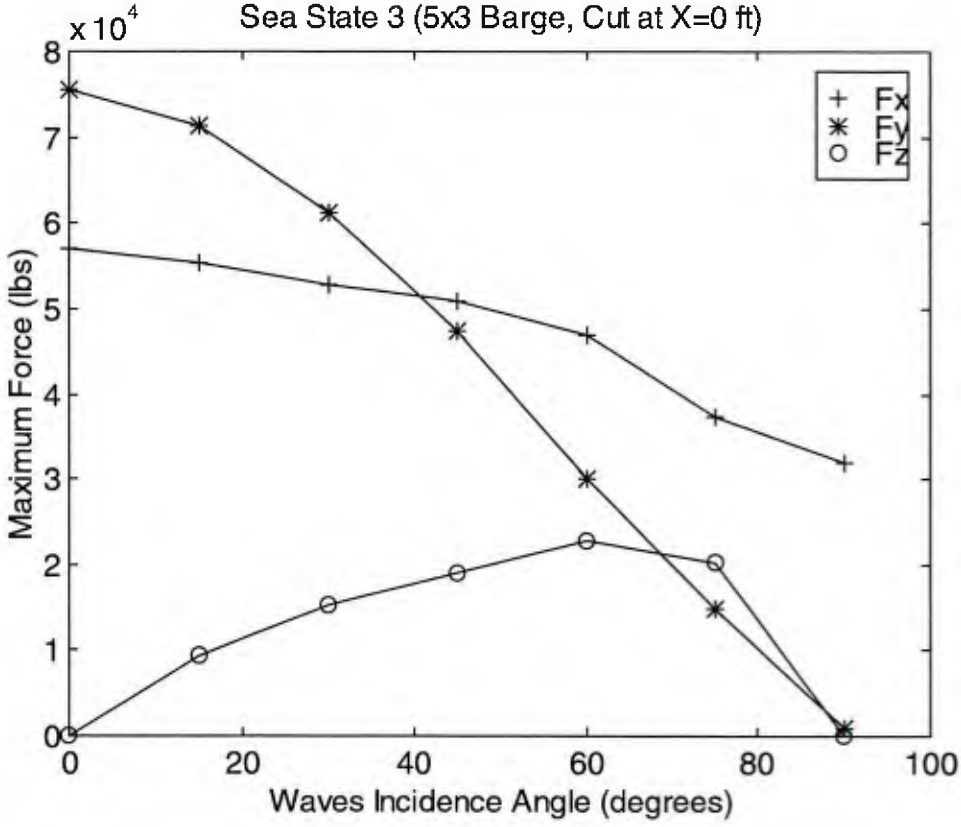

Figure 2.9 Maximum Section Forces at X=0 ft for the 5x3 Platform

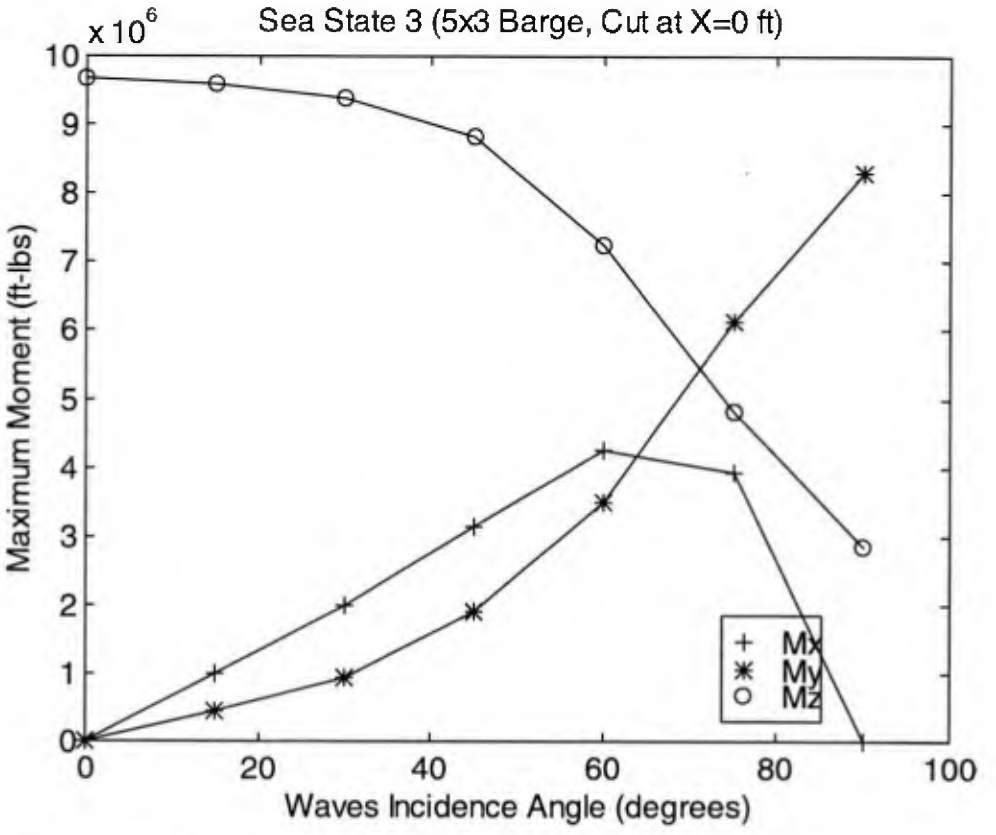

Figure 2.10 Maximum Section Bending Moments at X=0 ft for the 5x3 Platform

In summary, only the force component F_y and bending moment component M_z will be shown in the following section for all the cases with free bodies cut by vertical plane at X = constant ft. Based on the same reasons, only the force component, F_y, and bending moment component, M_x, will be shown in the following section for all the cases with free bodies cut by vertical plane at Z = constant ft. Note that all three of the force components and three bending moment components were computed and kept in file if they were required for design or verification purposes.

2.6 Results of Parametric Study (F_y, M_x, and M_z)

The following figures show the comparison of the force component, F_y, and bending moment components, M_z and M_x, at various imaginary cut locations for different platform sizes in both operational seas (SS3) and survival seas (SS5). As described in the previous section, the wave direction varies from 0 degrees to 90 degrees with an increment of 15 degrees. Comparisons may be drawn for these cases by studying each figure and its associated legend.

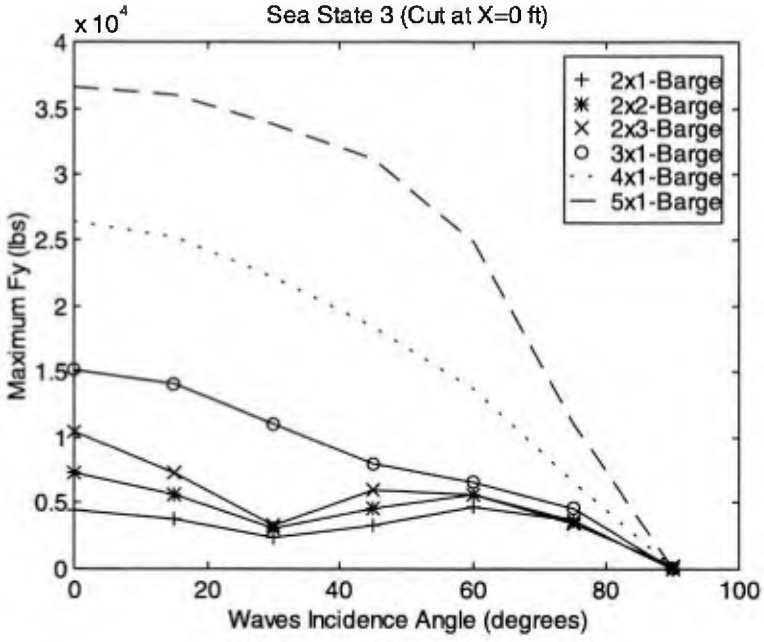

Figure 2.11 Comparison of F_y

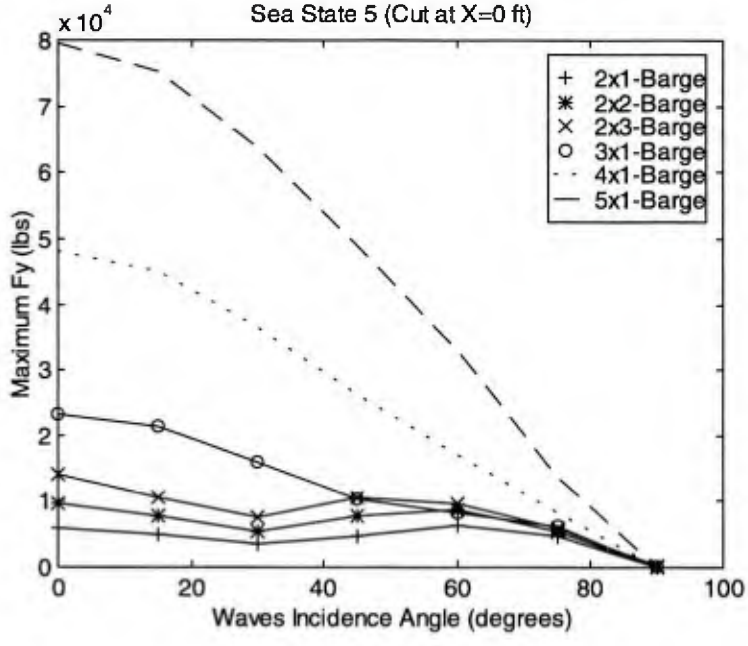

Figure 2.12 Comparison of F_y

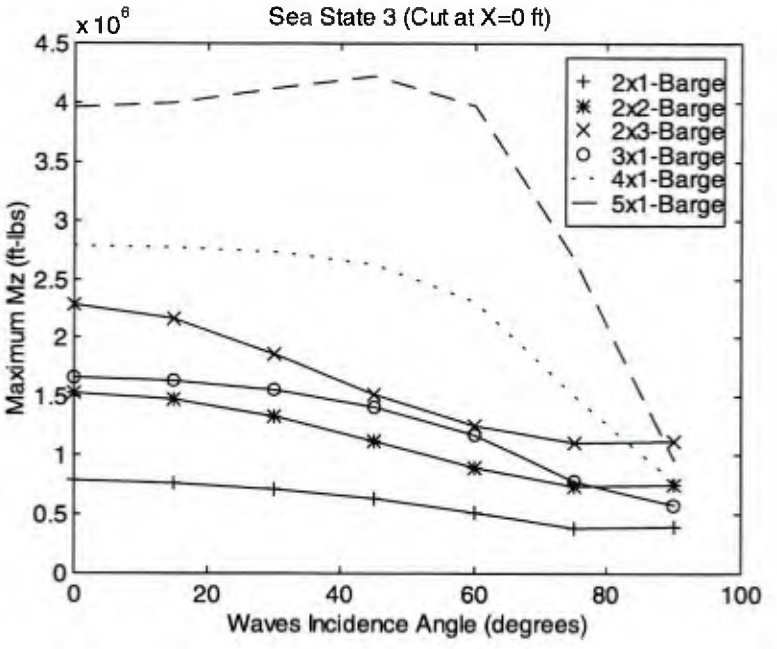

Figure 2.13 Comparison of M_z

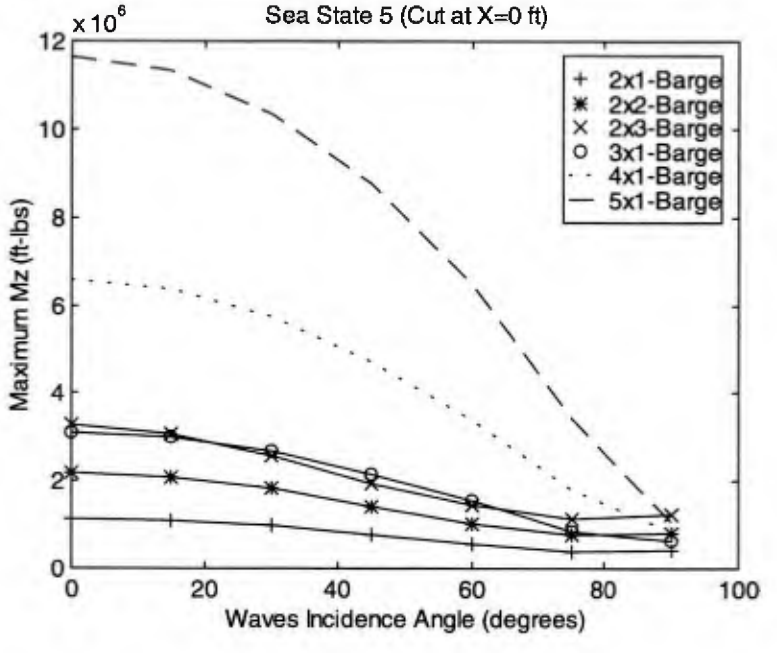

Figure 2.14 Comparison of M_z

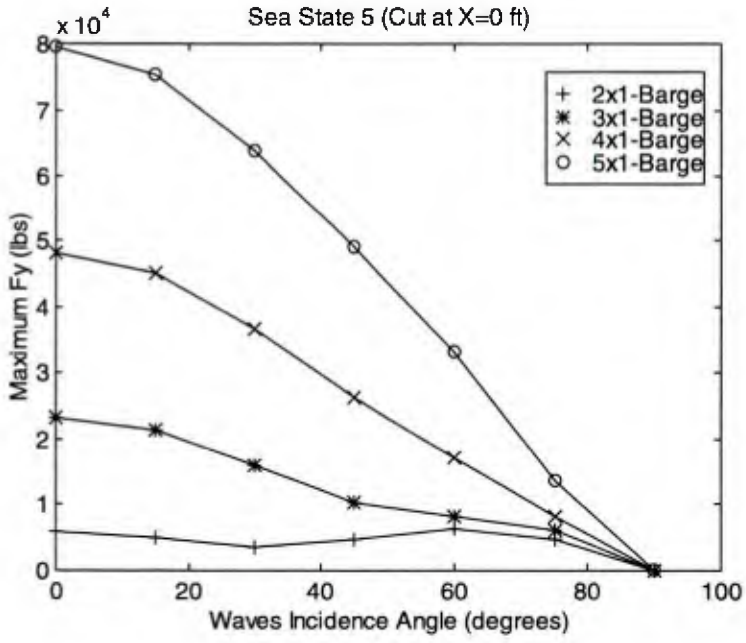

Figure 2.15 Comparison of F_y

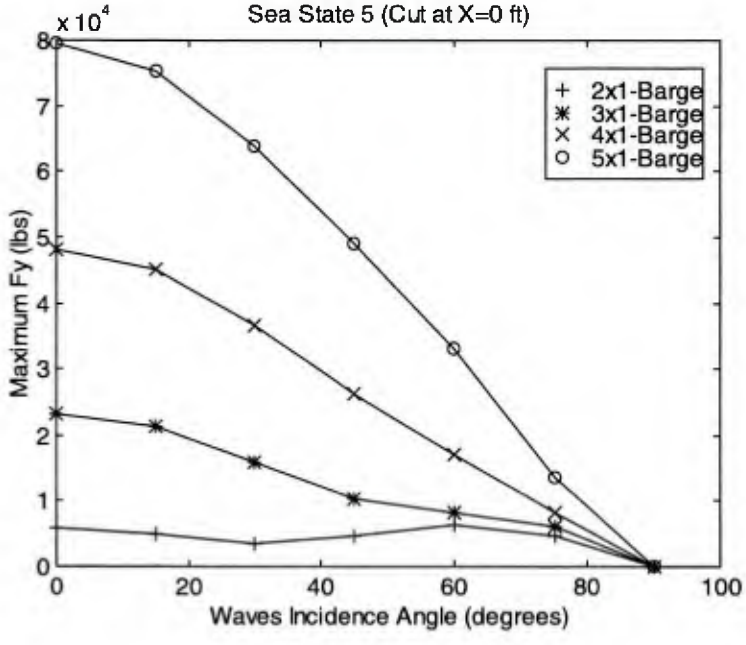

Figure 2.16 Comparison of F_y

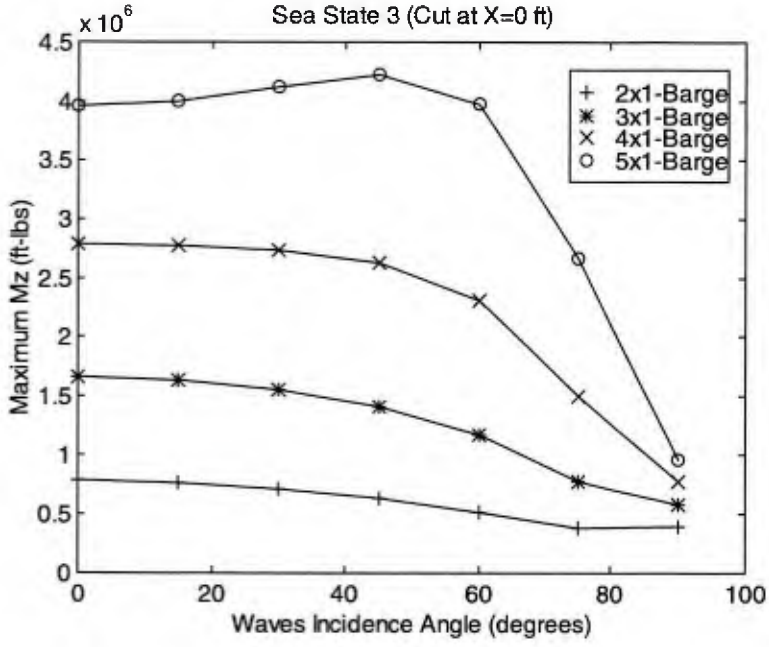

Figure 2.17 Comparison of M_z

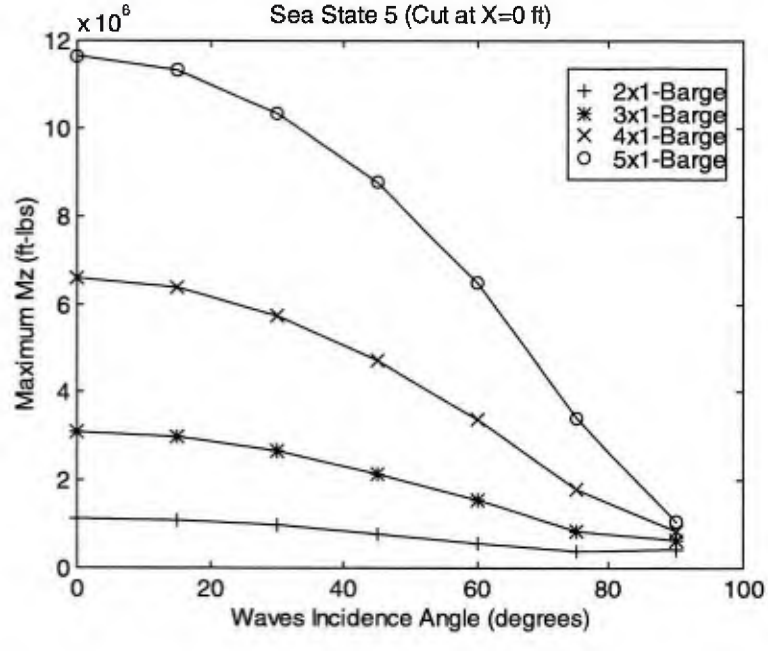

Figure 2.18 Comparison of M_z

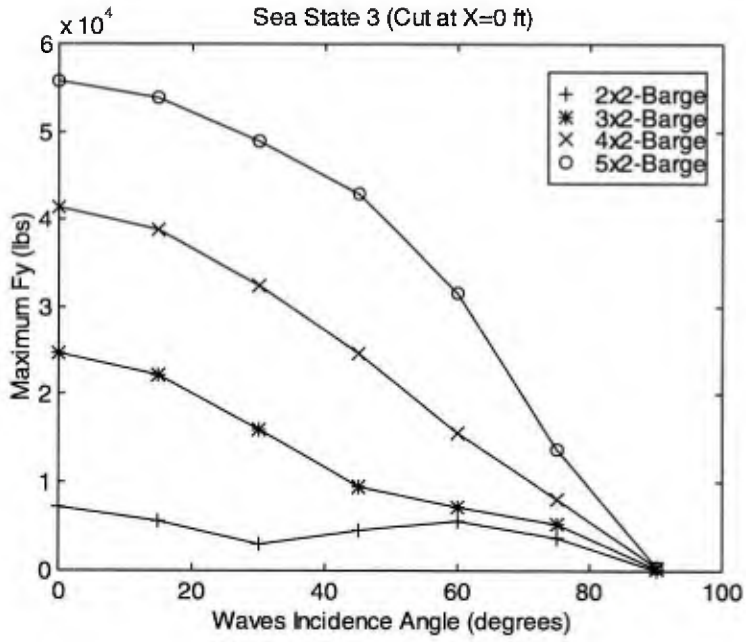

Figure 2.19 Comparison of F_y

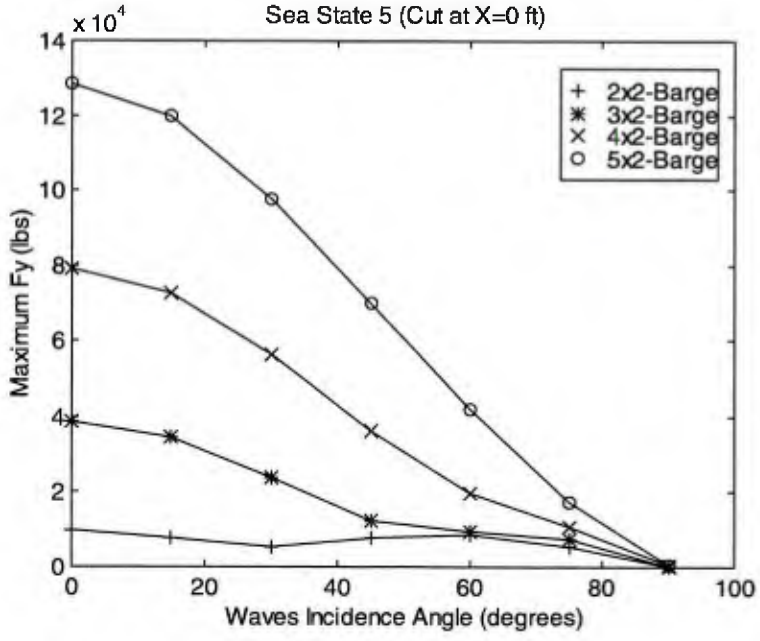

Figure 2.20 Comparison of F_y

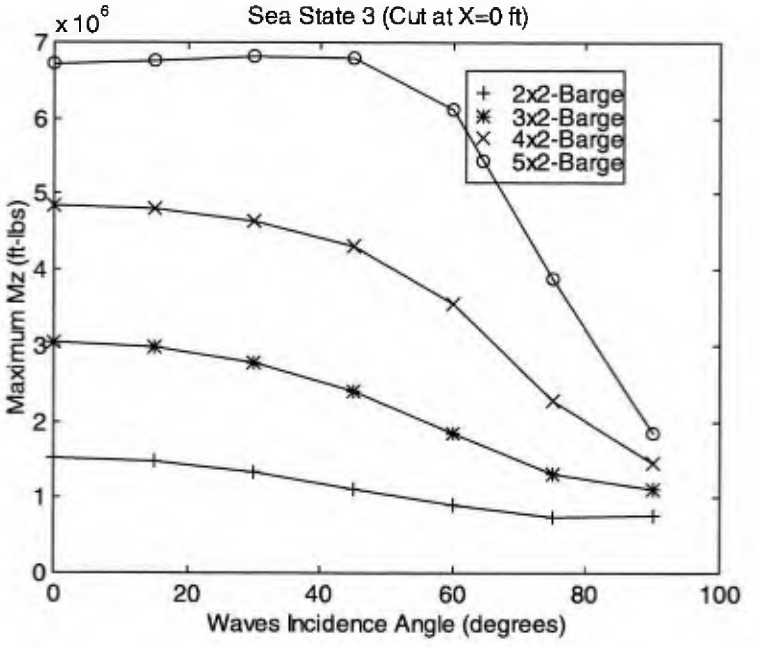

Figure 2.21 Comparison of M_z

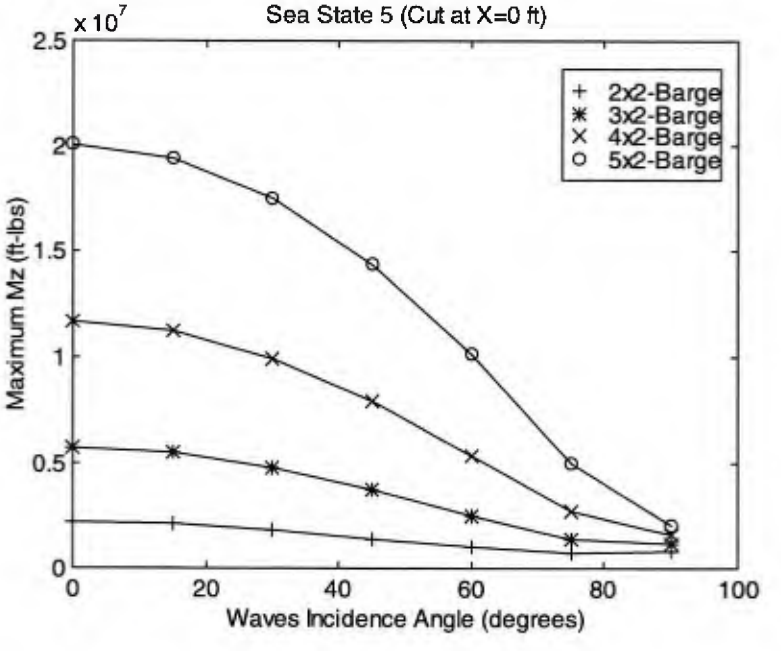

Figure 2.22 Comparison of M_z

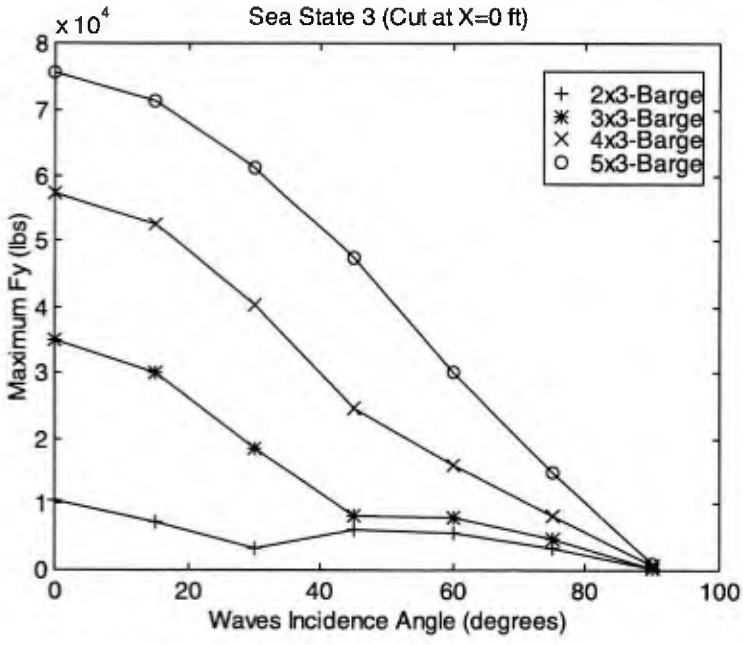

Figure 2.23 Comparison of F_y

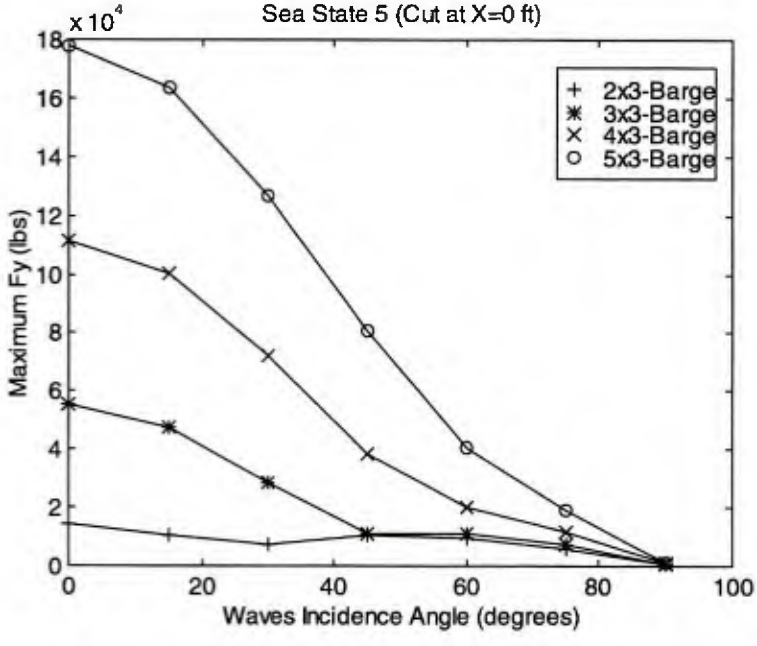

Figure 2.24 Comparison of F_y

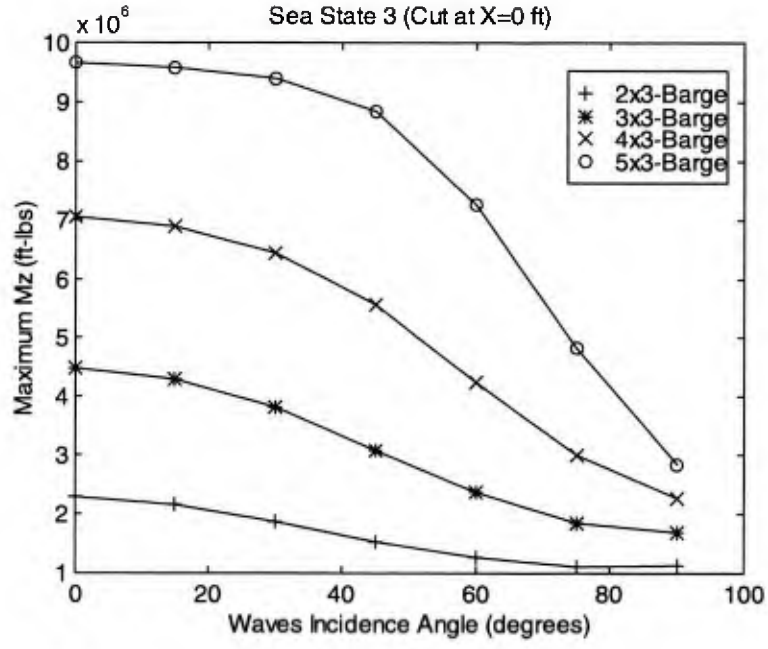

Figure 2.25 Comparison of M_z

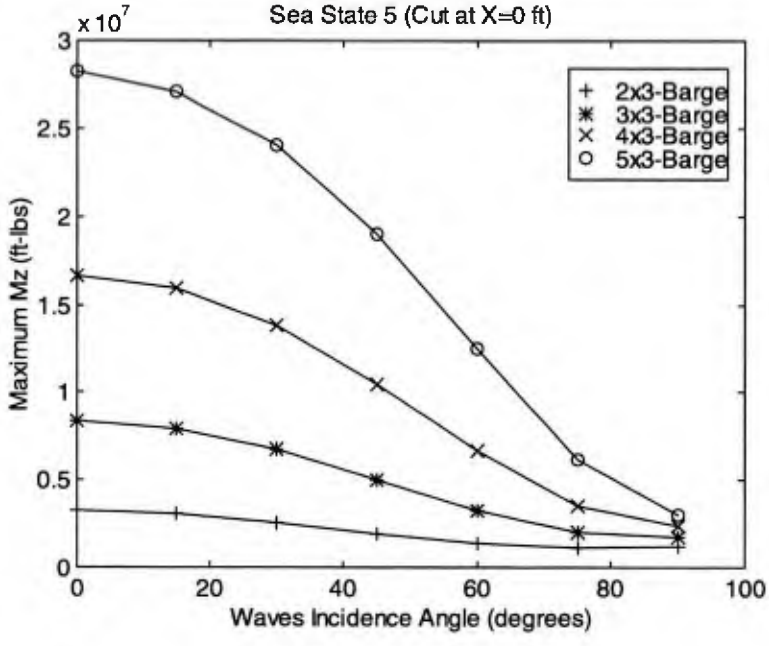

Figure 2.26 Comparison of M_z

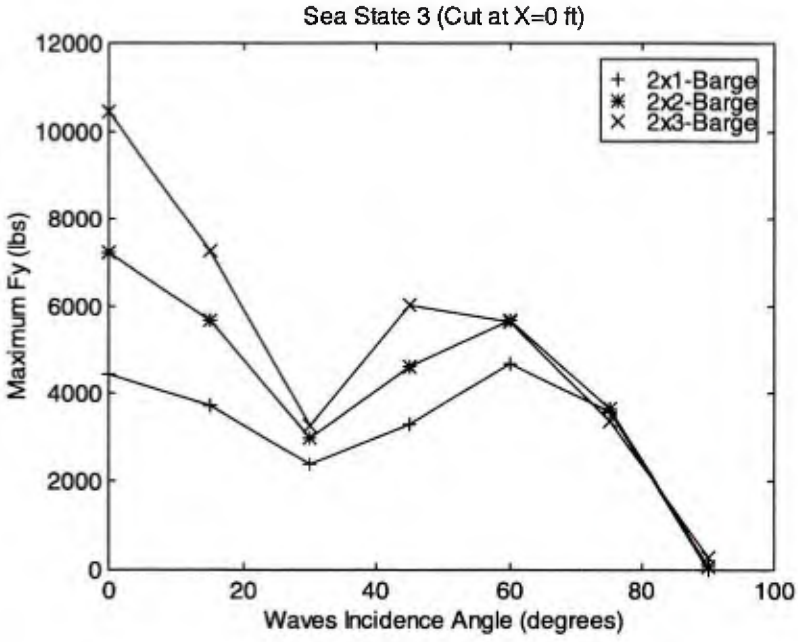

Figure 2.27 Comparison of F_y

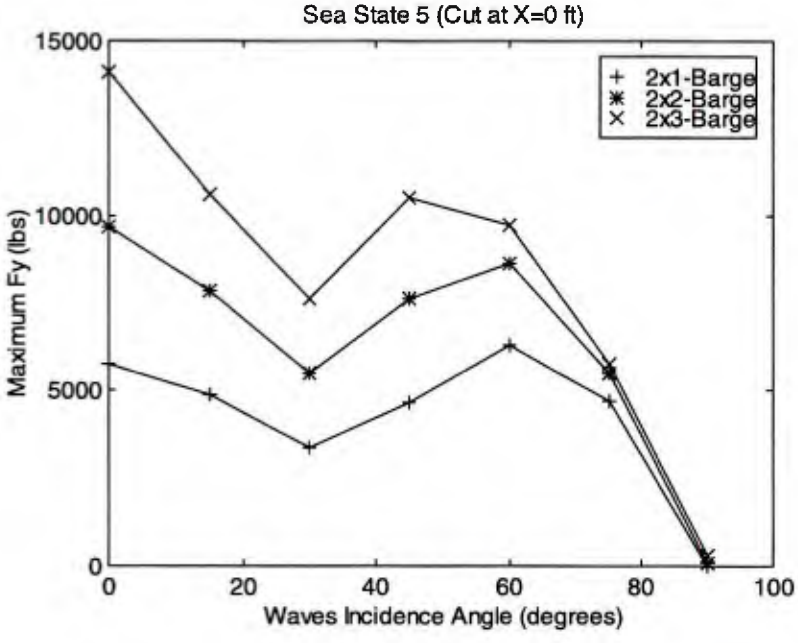

Figure 2.28 Comparison of F_y

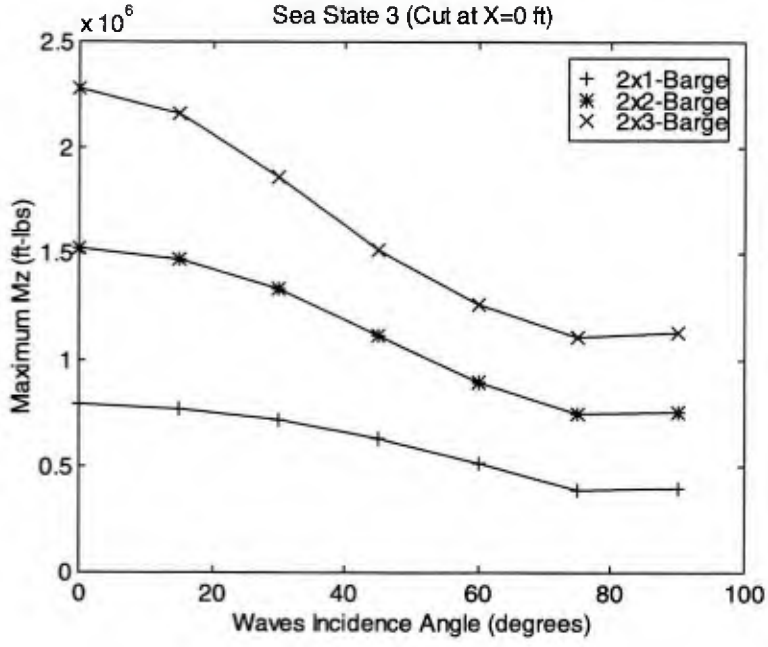

Figure 2.29 Comparison of M_z

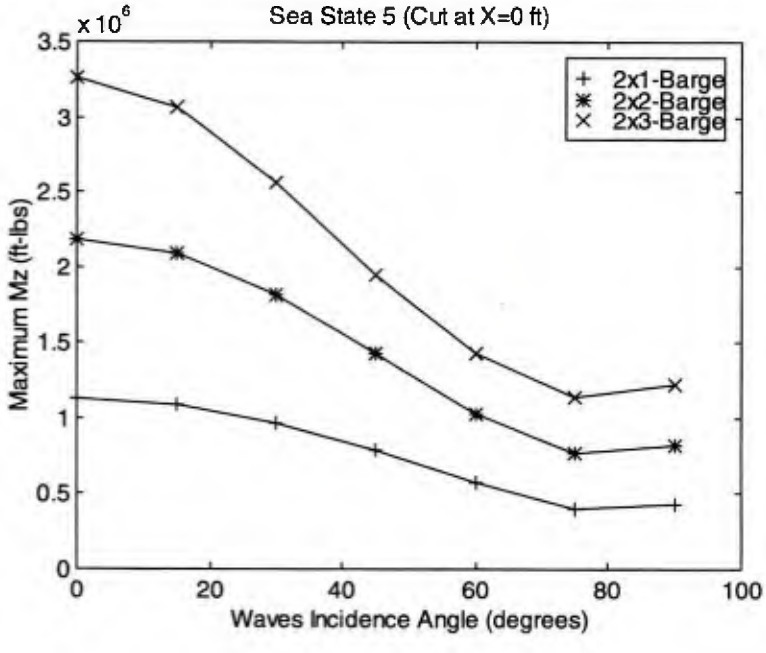

Figure 2.30 Comparison of M_z

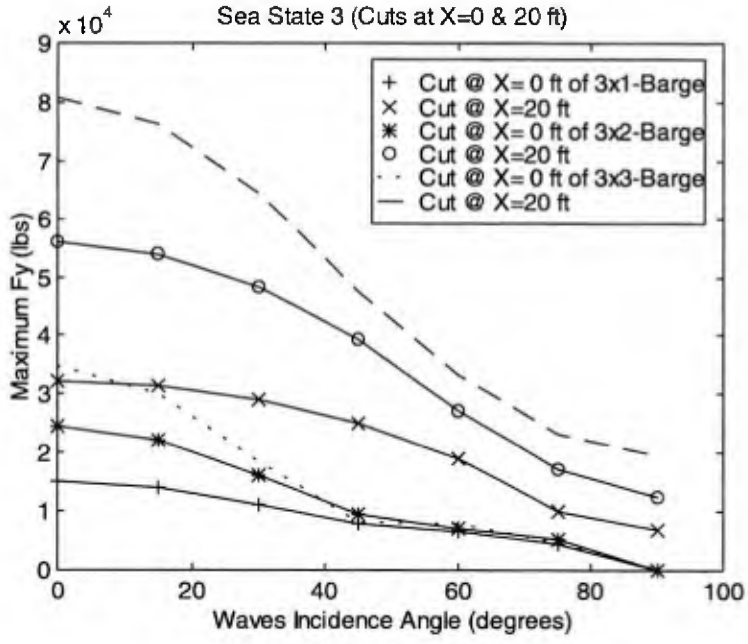

Figure 2.31 Comparison of F_y

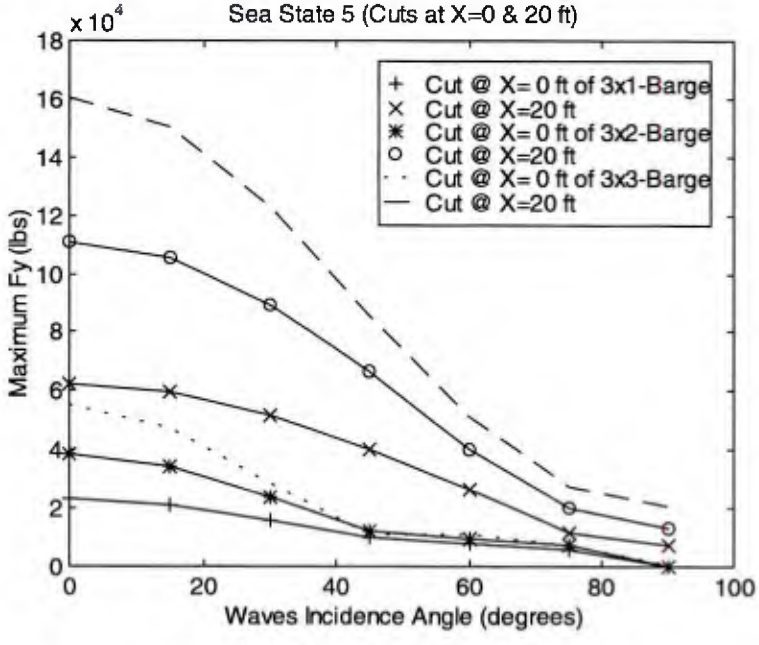

Figure 2.32 Comparison of F_y

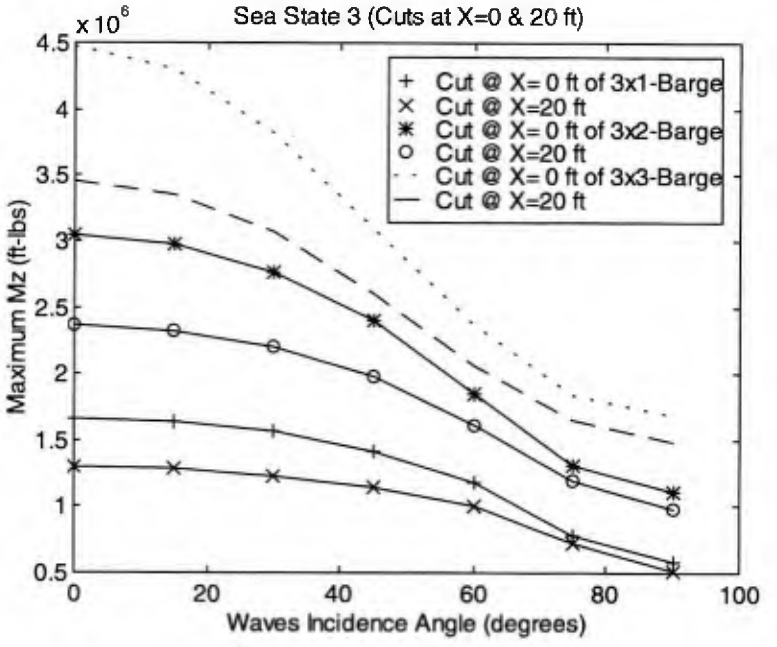

Figure 2.33 Comparison of M_z

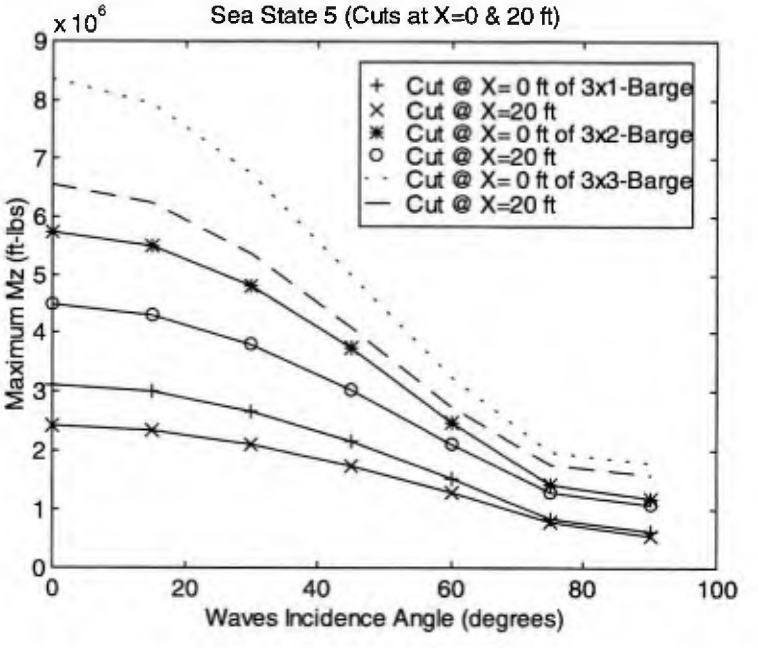

Figure 2.34 Comparison of M_z

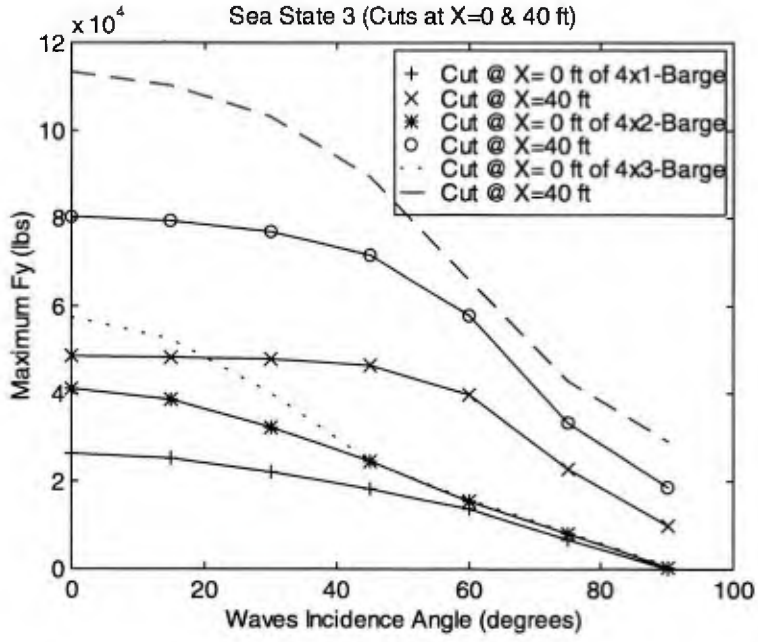

Figure 2.35 Comparison of F_y

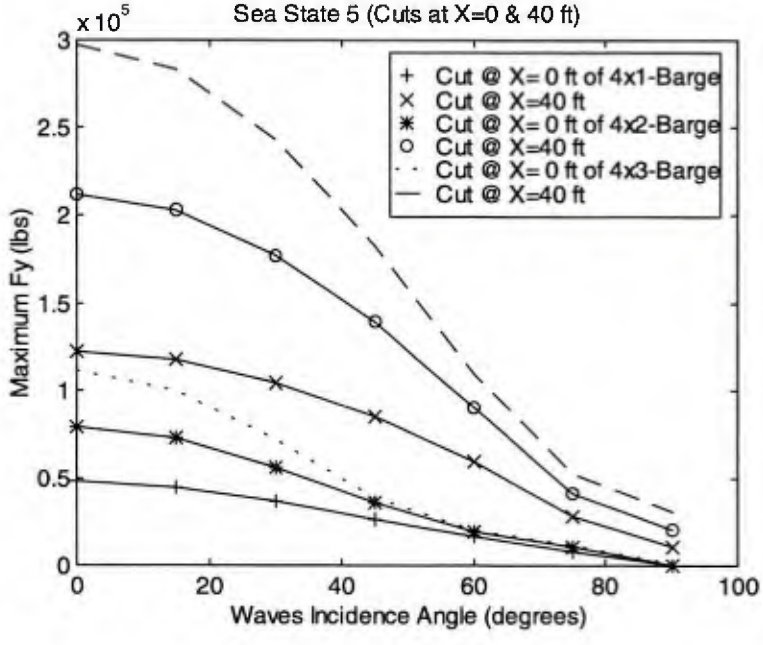

Figure 2.36 Comparison of F_y

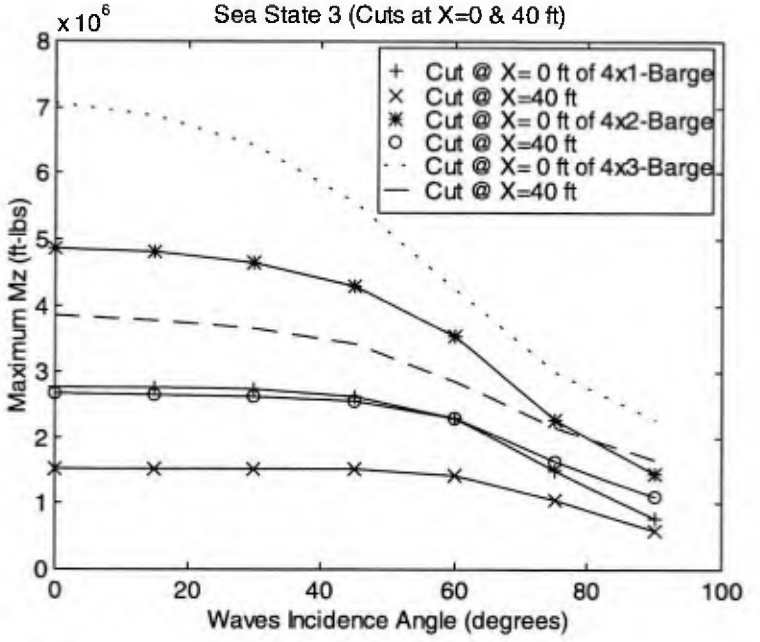

Figure 2.37 Comparison of M_z

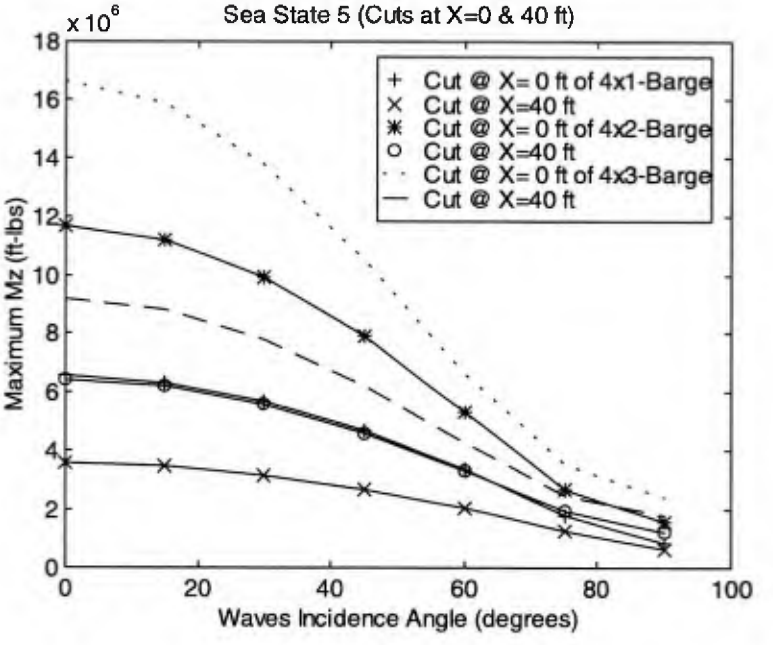

Figure 2.38 Comparison of M_z

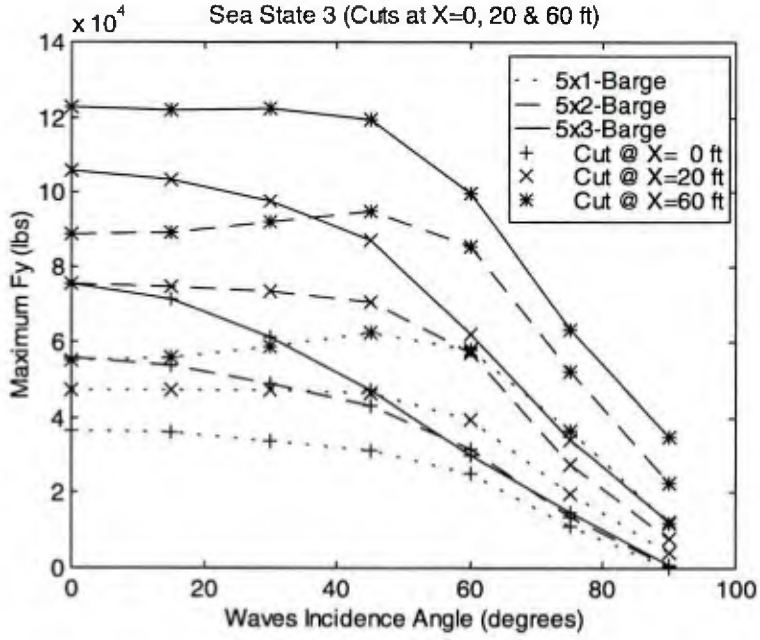

Figure 2.39 Comparison of F_y

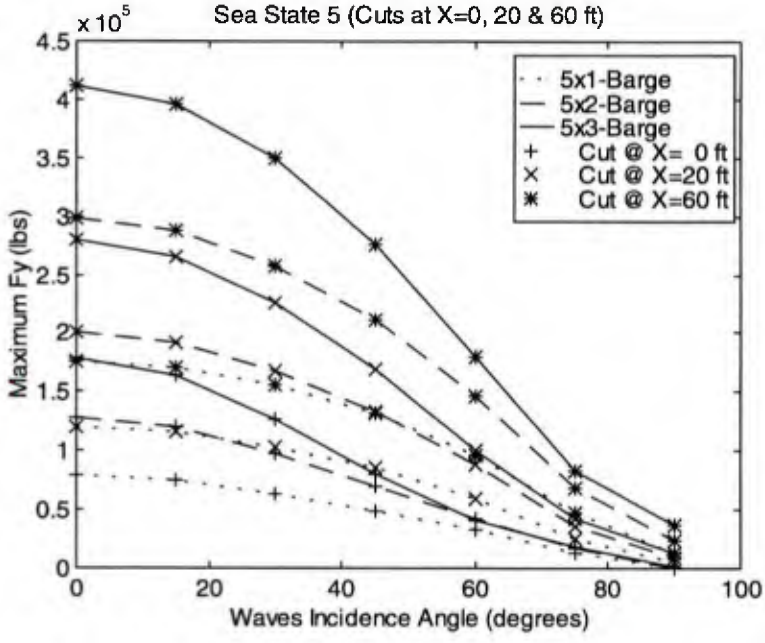

Figure 2.40 Comparison of F_y

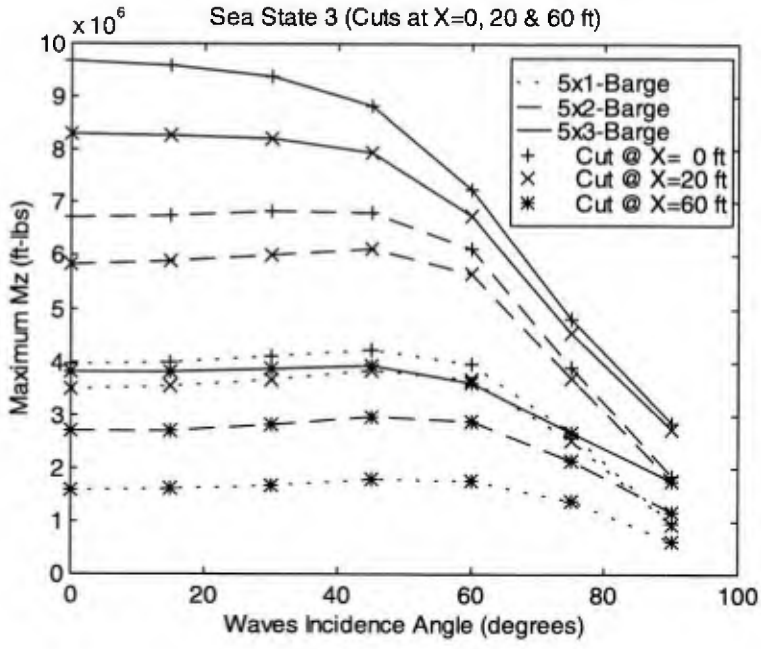

Figure 2.41 Comparison of M_z

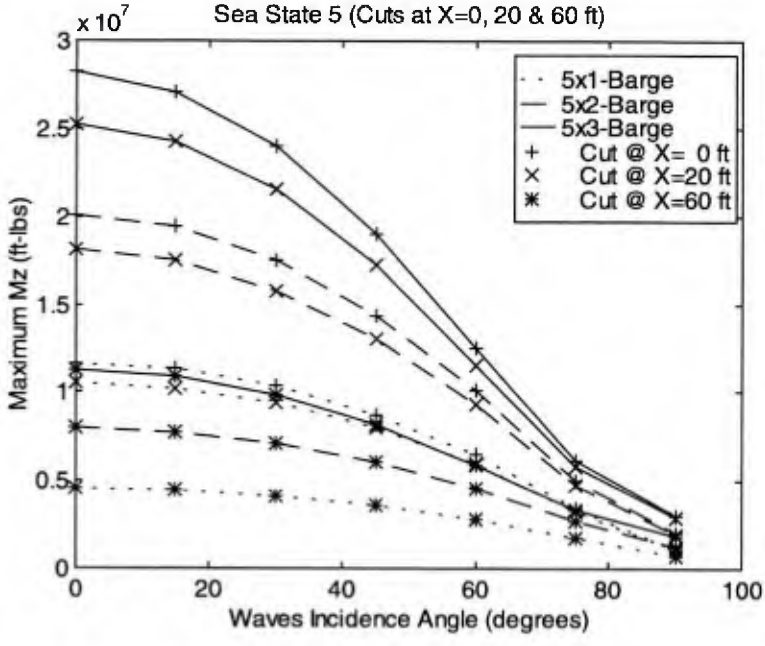

Figure 2.42 Comparison of M_z

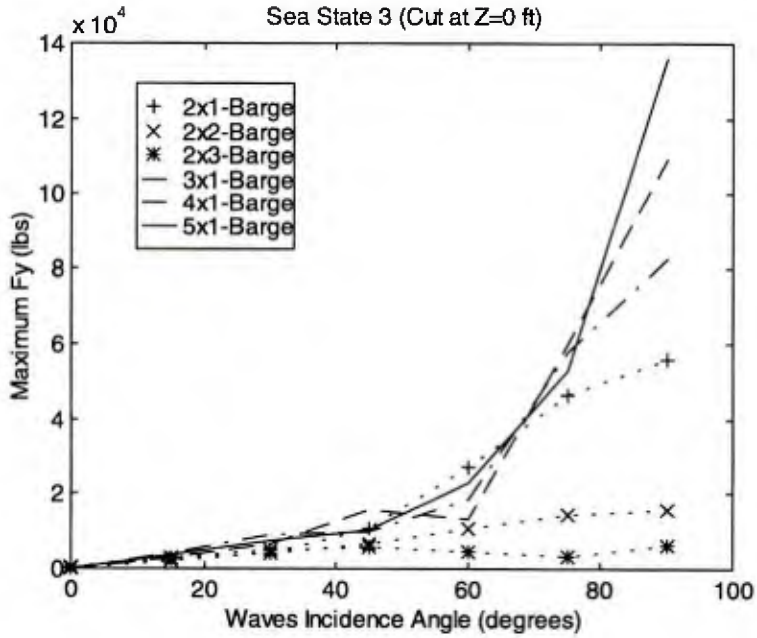

Figure 2.43 Comparison of F_y

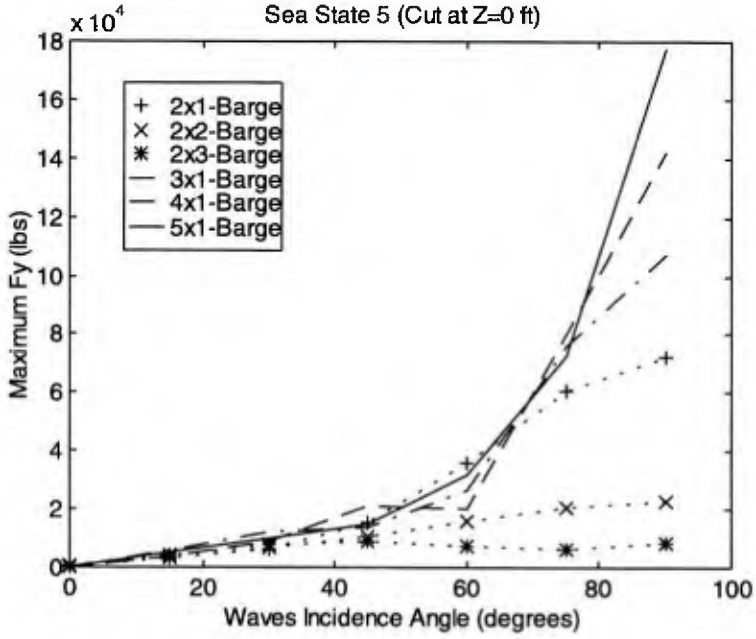

Figure 2.44 Comparison of F_y

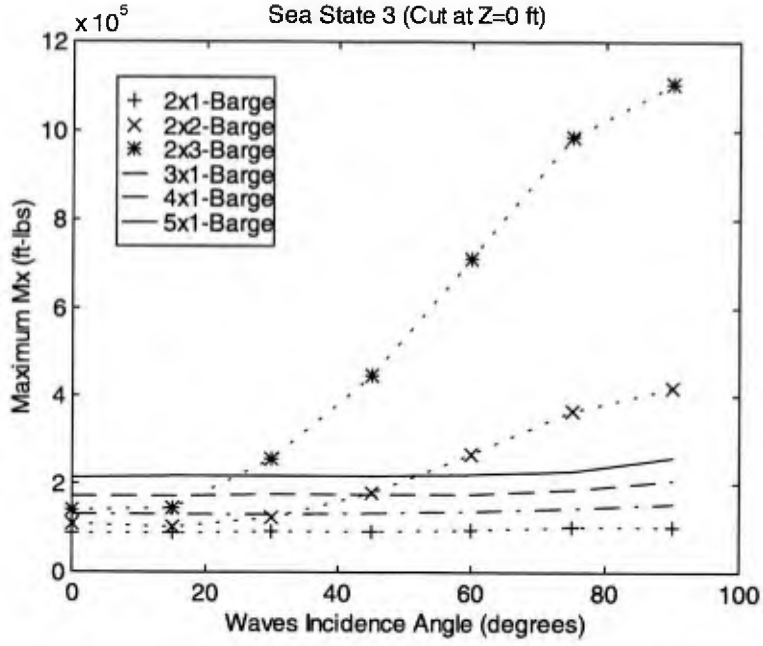

Figure 2.45 Comparison of M_x

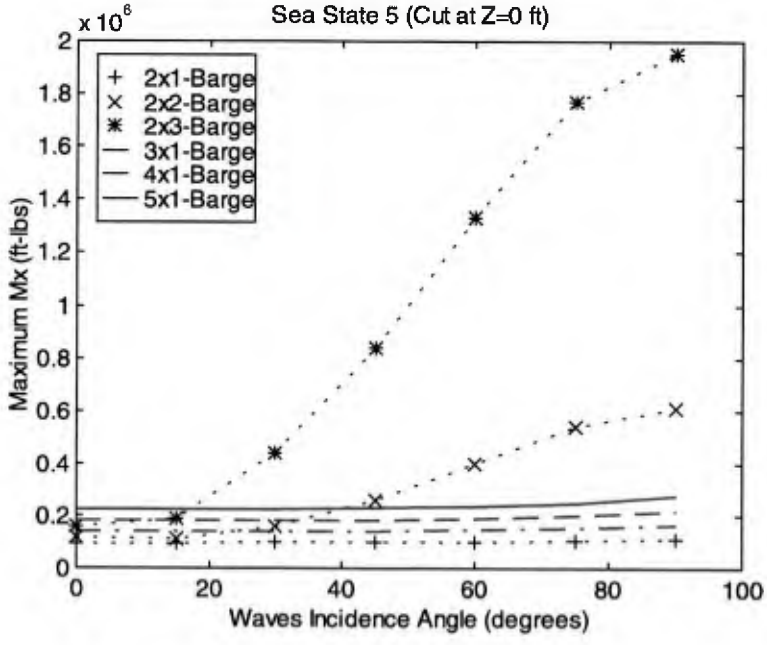

Figure 2.46 Comparison of M_x

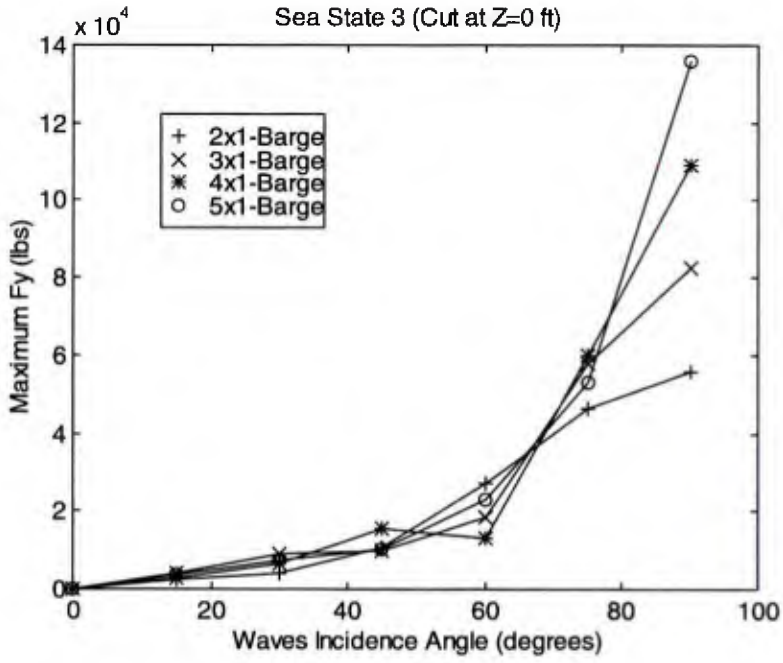

Figure 2.47 Comparison of F_y

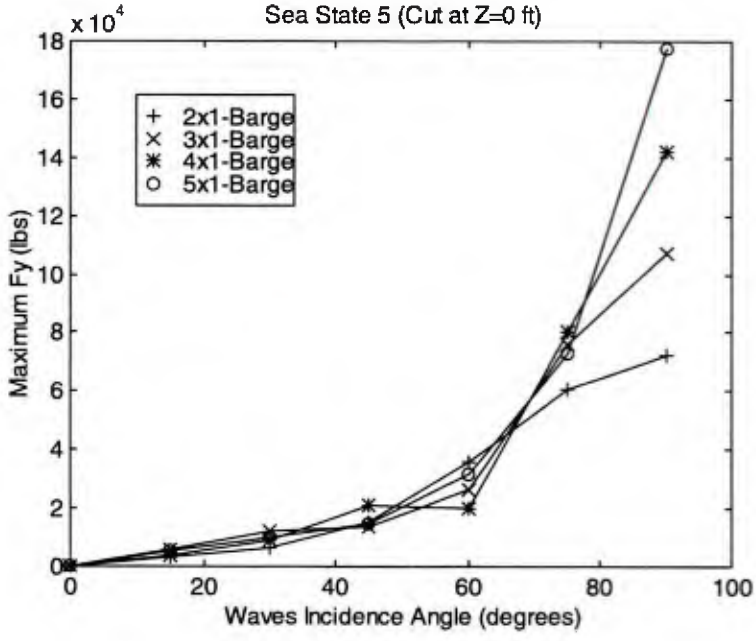

Figure 2.48 Comparison of F_y

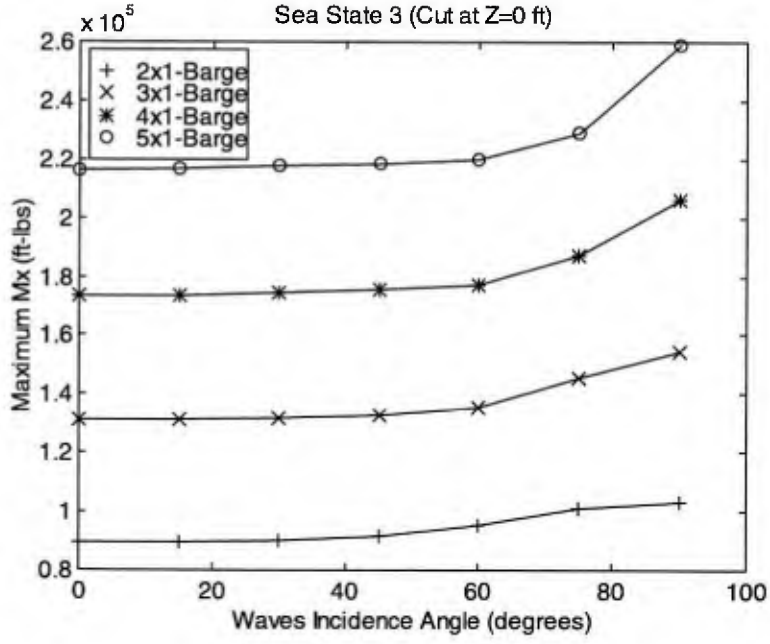

Figure 2.49 Comparison of M_x

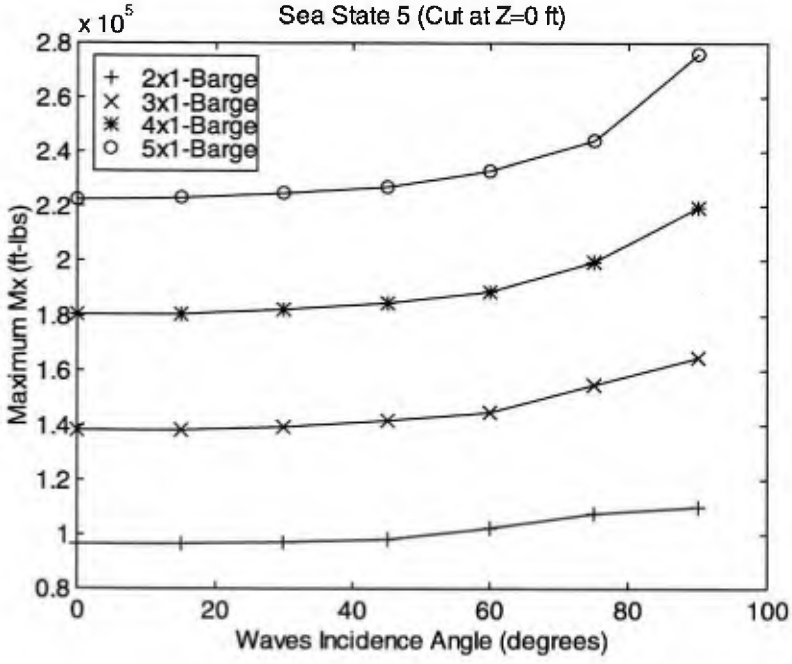

Figure 2.50 Comparison of M_x

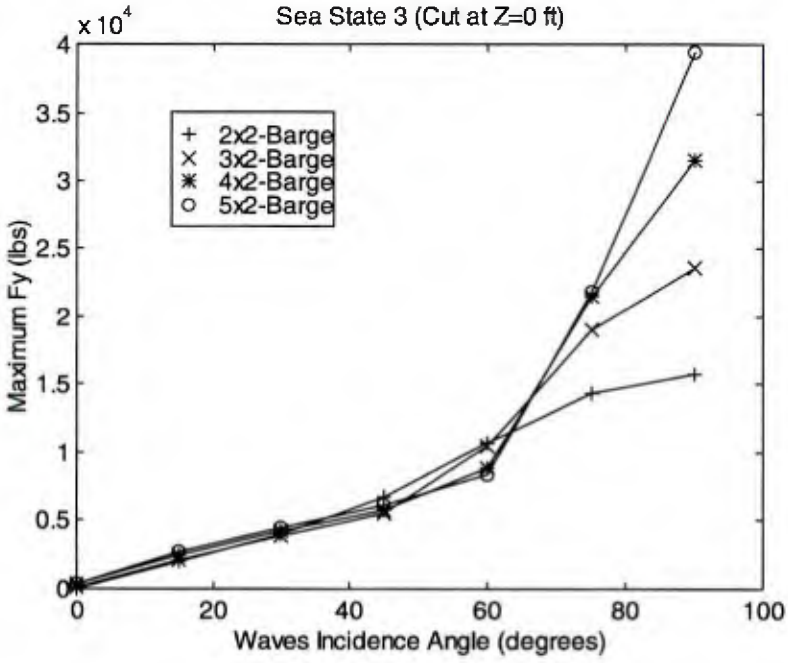

Figure 2.51 Comparison of F_y

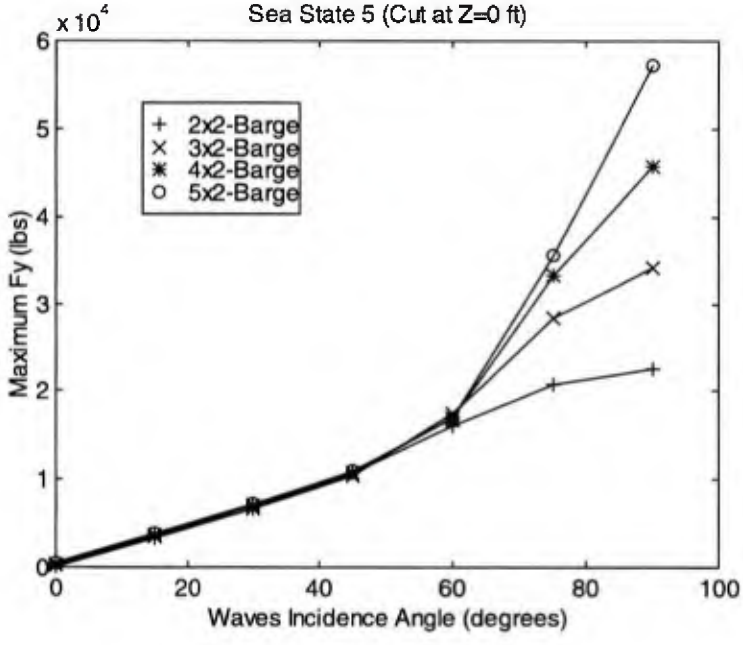

Figure 2.52 Comparison of F_y

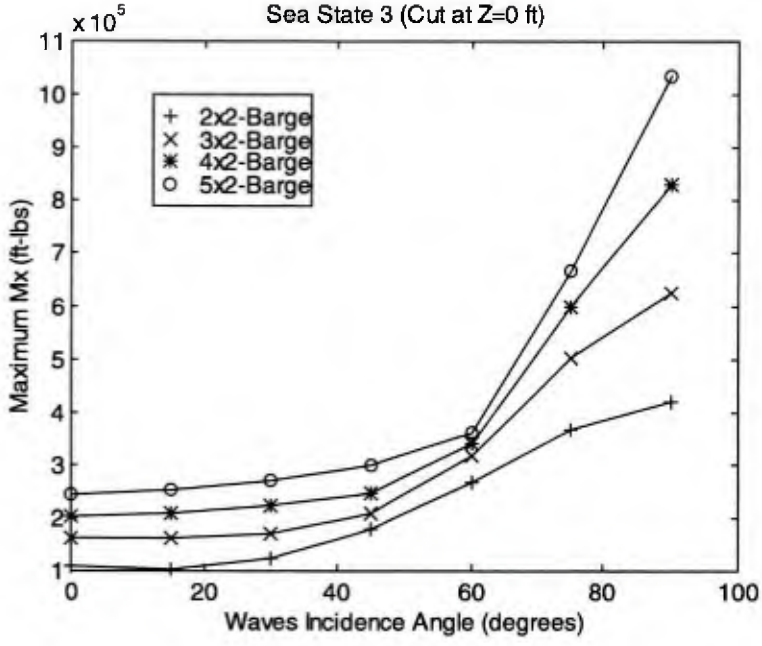

Figure 2.53 Comparison of M_x

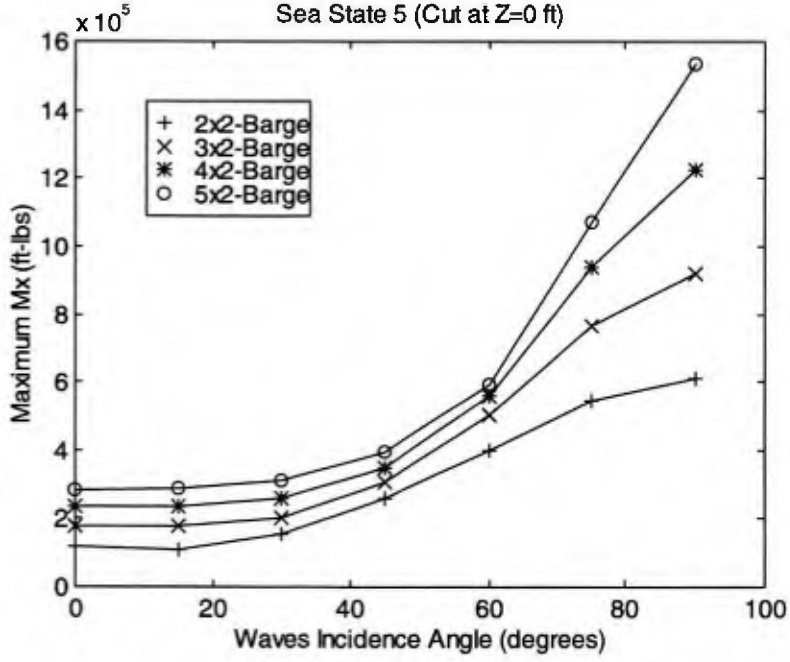

Figure 2.54 Comparison of M_x

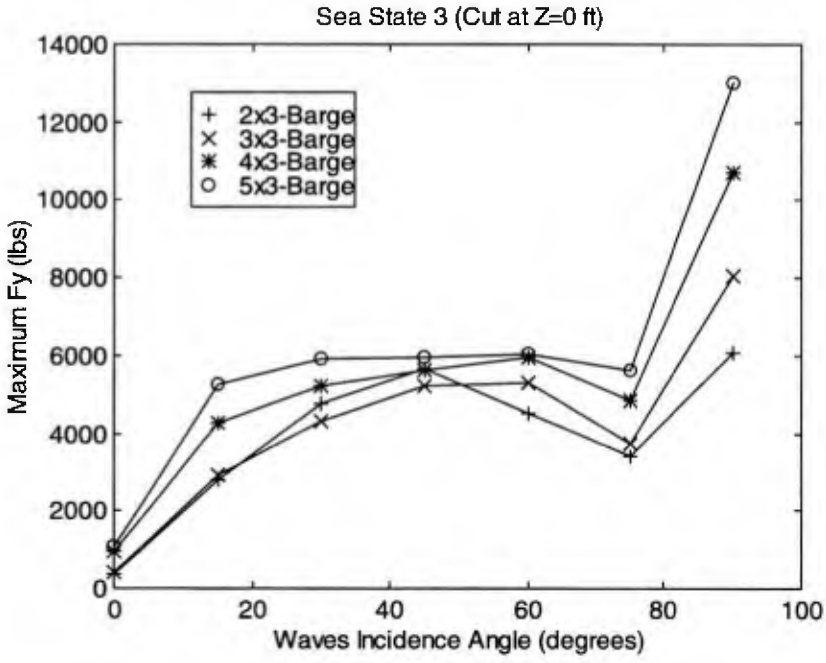

Figure 2.55 Comparison of F_y

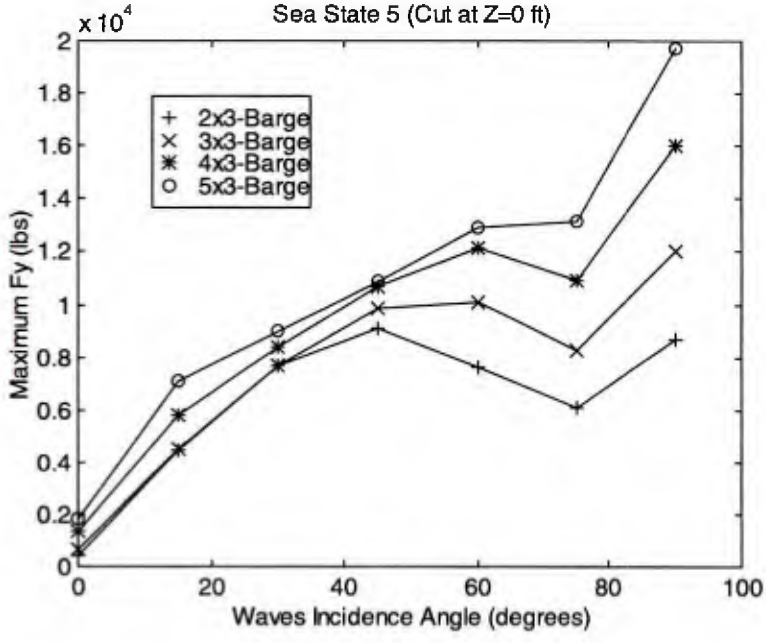

Figure 2.56 Comparison of F_y

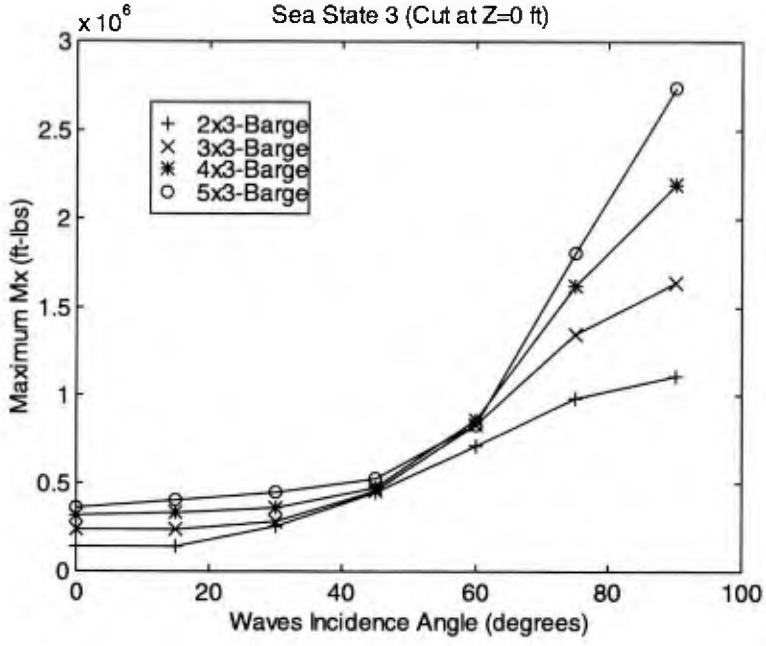

Figure 2.57 Comparison of M_x

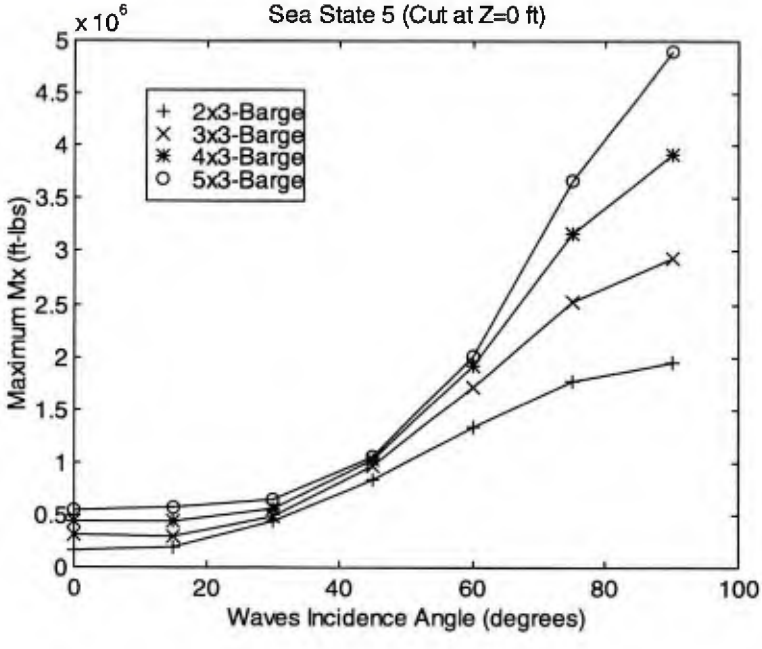

Figure 2.58 Comparison of M_x

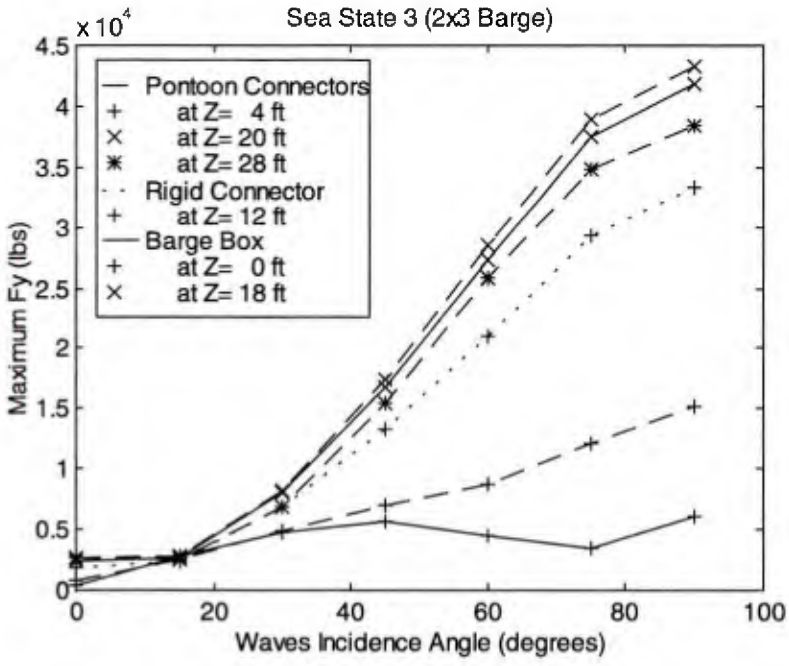

Figure 2.59 Comparison of F_y

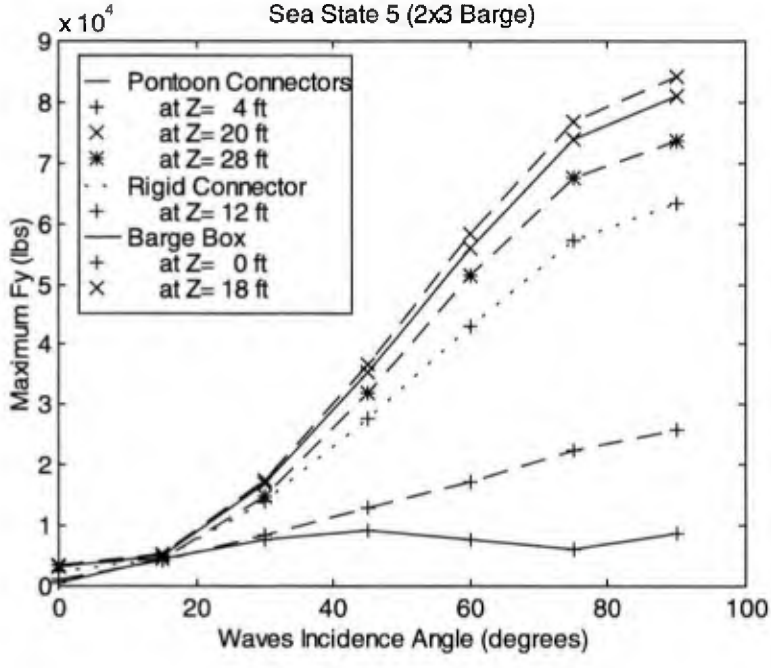

Figure 2.60 Comparison of F_y

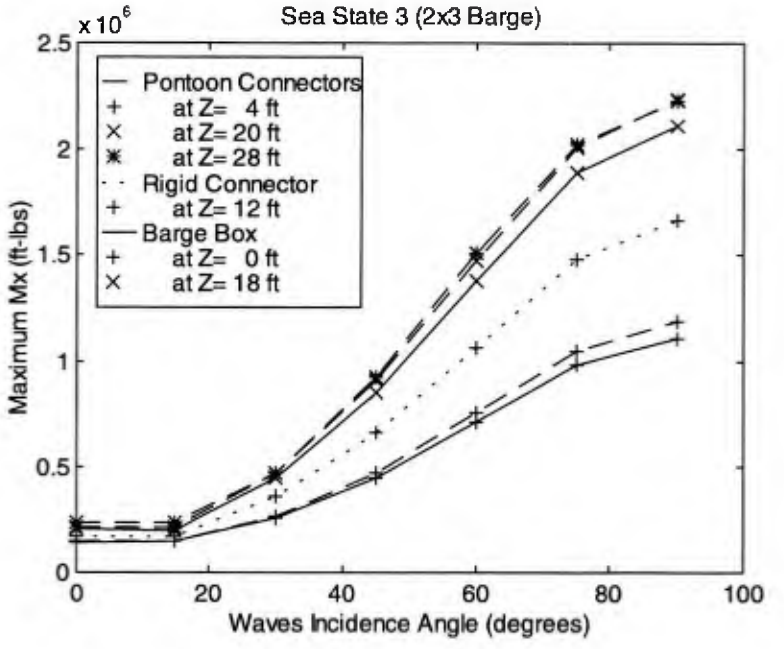

Figure 2.61 Comparison of M_x

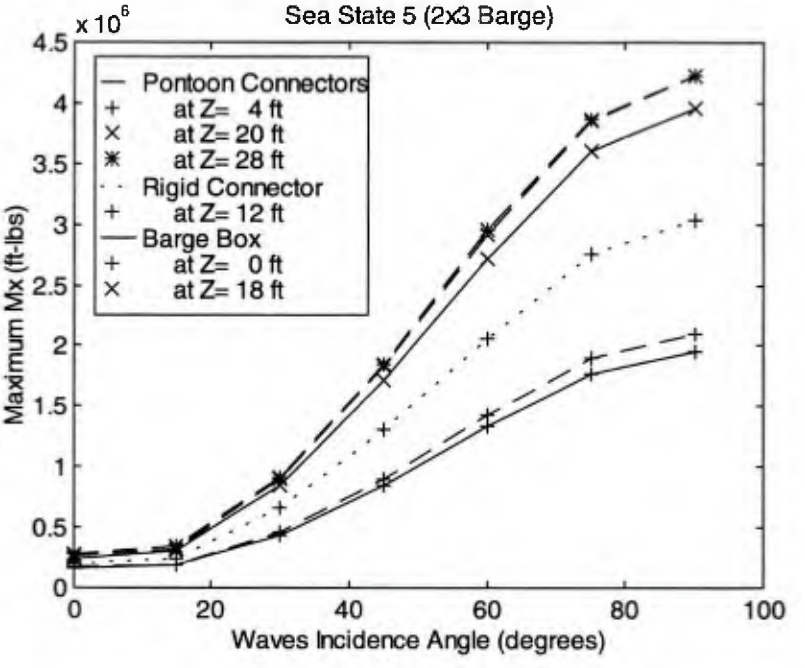

Figure 2.62 Comparison of M_x

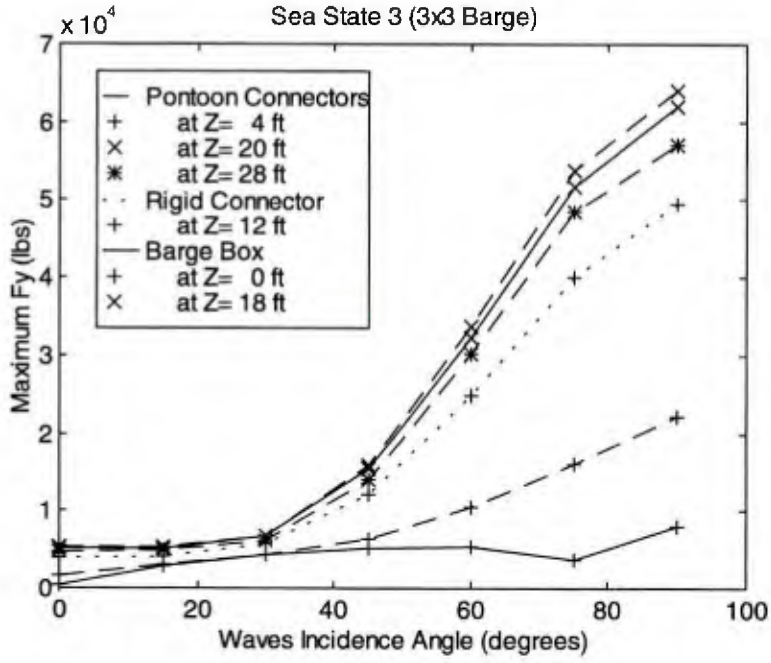

Figure 2.63 Comparison of F_y

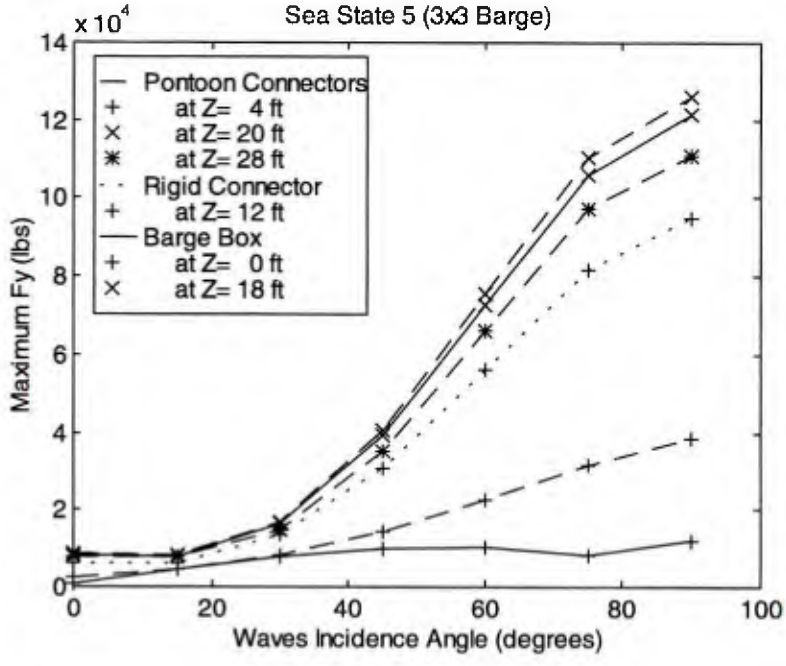

Figure 2.64 Comparison of F_y

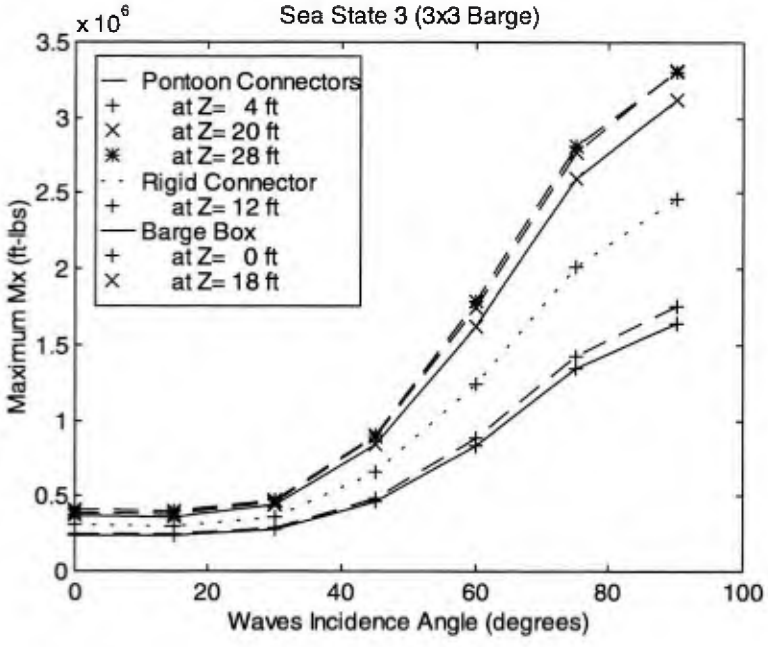

Figure 2.65 Comparison of M_x

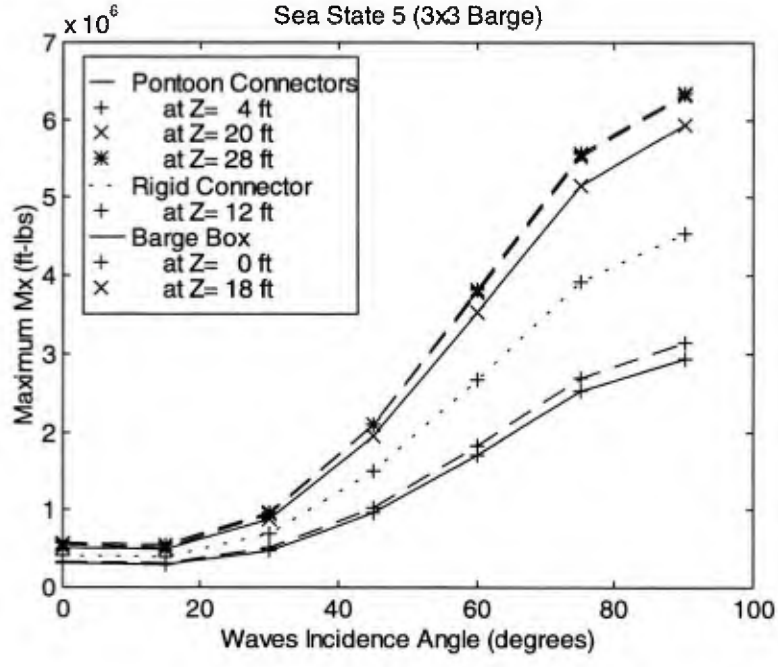

Figure 2.66 Comparison of M_x

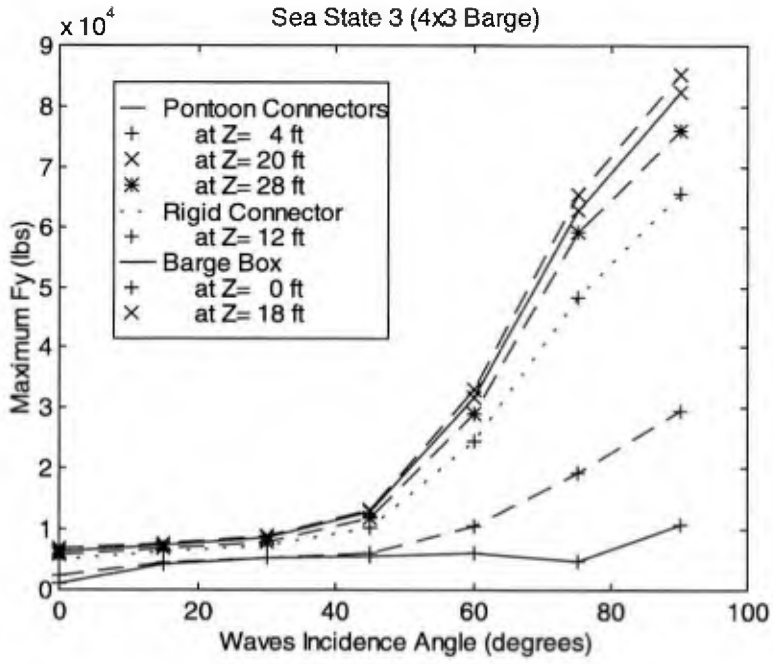

Figure 2.67 Comparison of F_y

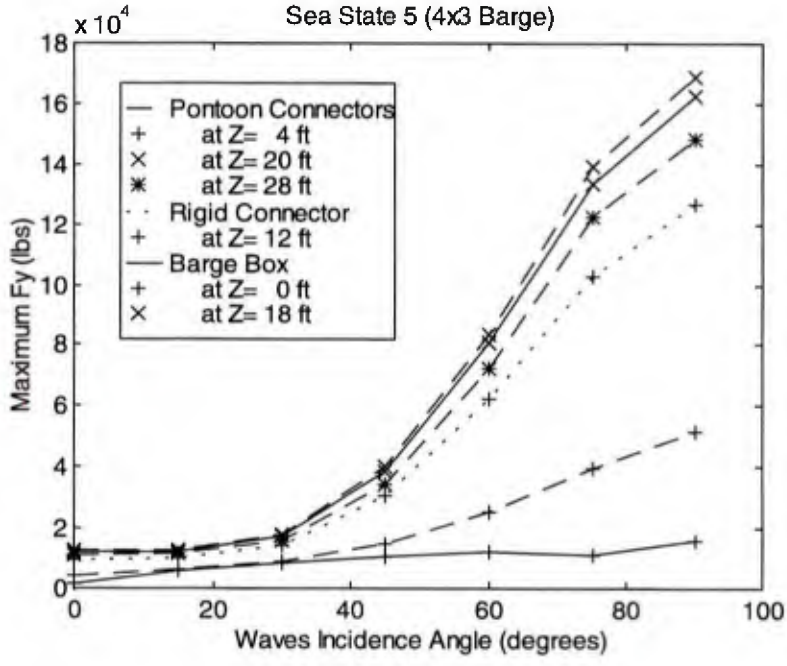

Figure 2.68 Comparison of F_y

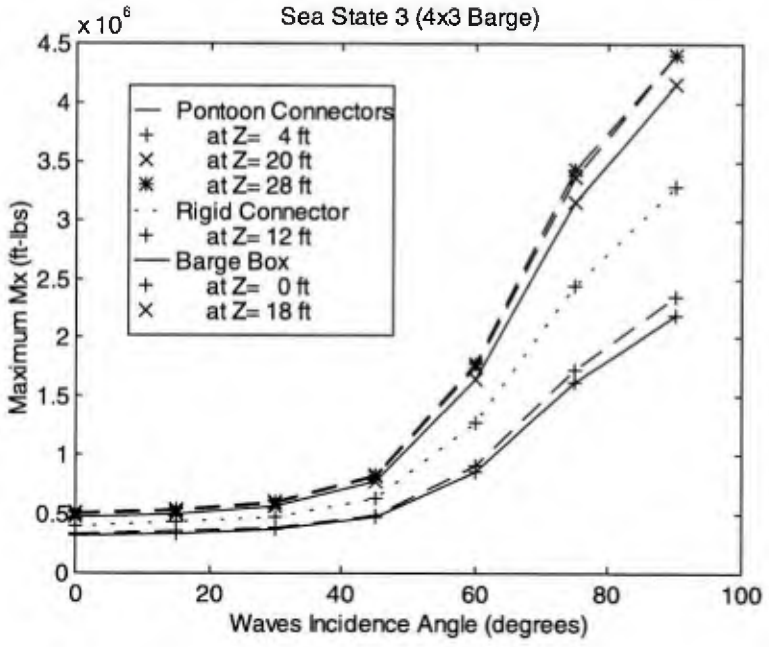

Figure 2.69 Comparison of M_x

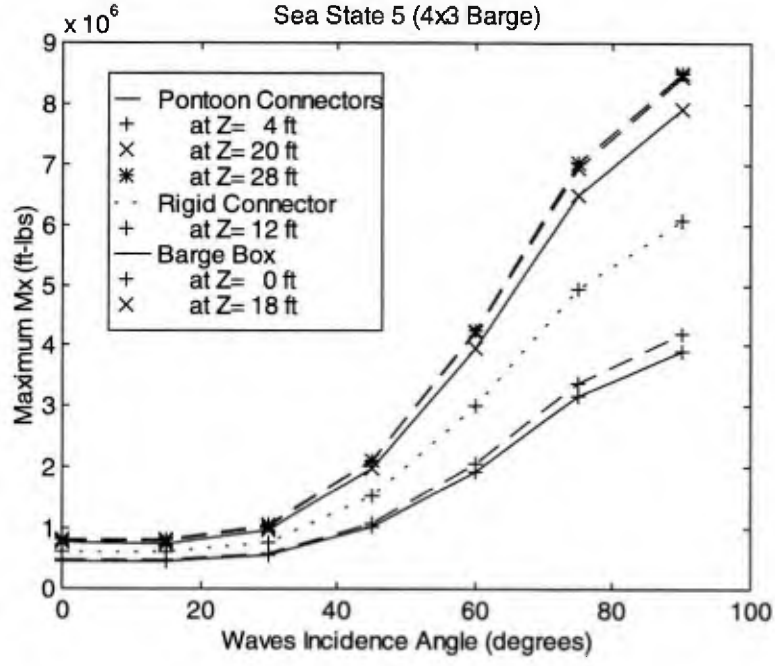

Figure 2.70 Comparison of M_x

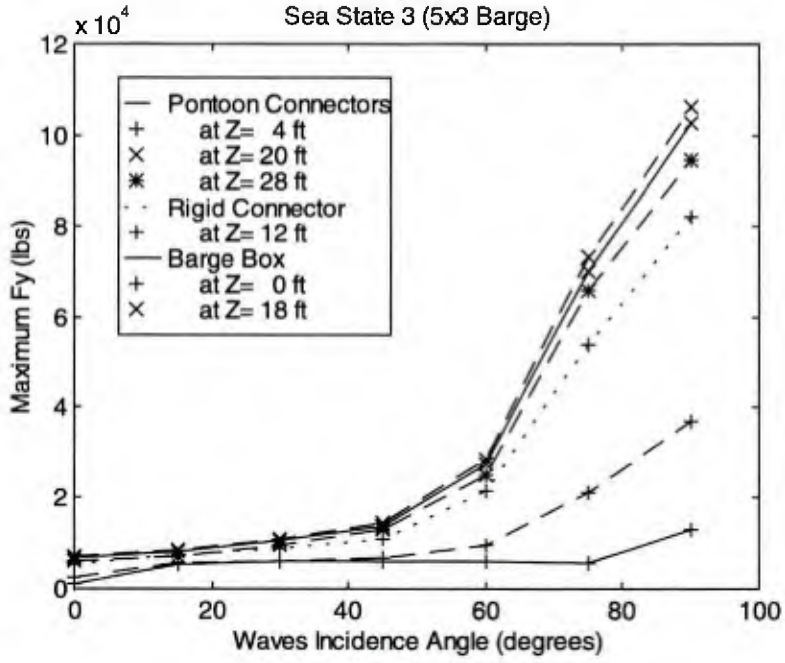

Figure 2.71 Comparison of F_y

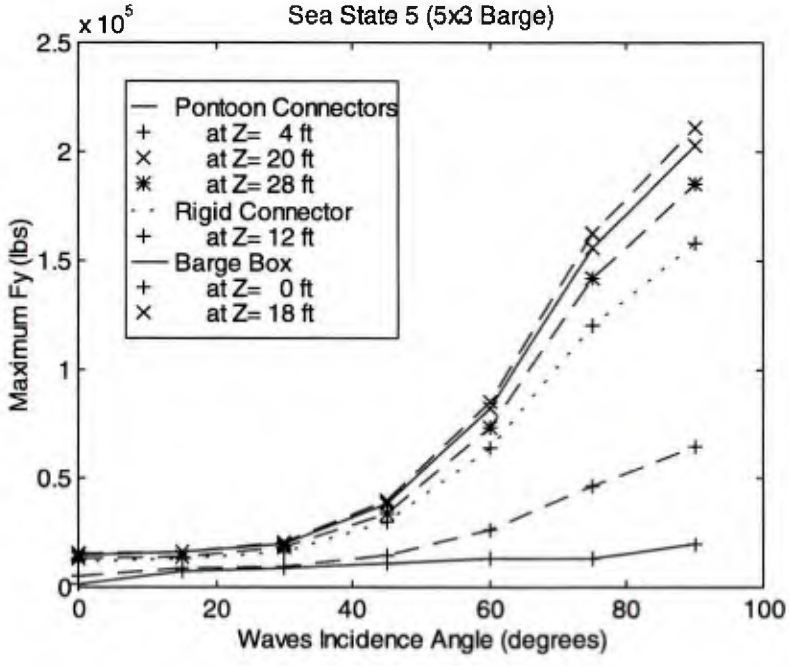

Figure 2.72 Comparison of F_y

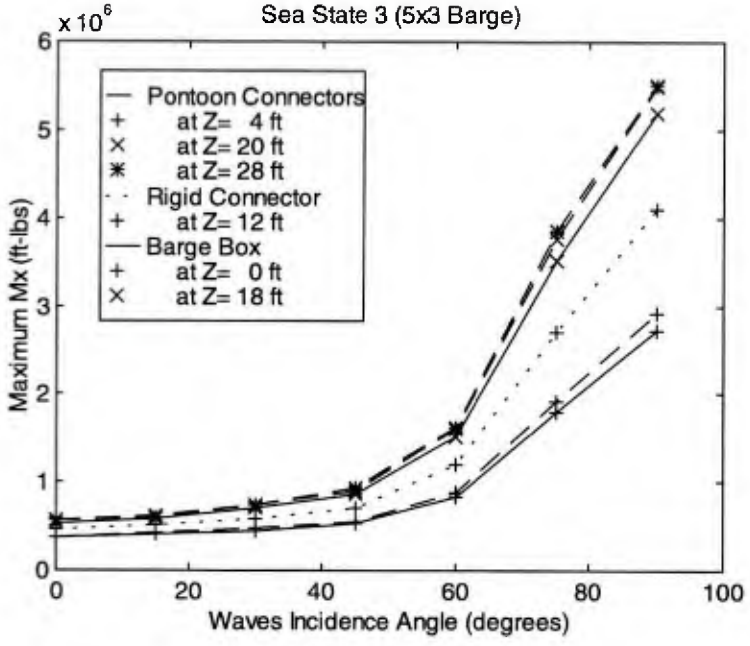

Figure 2.73 Comparison of M_x

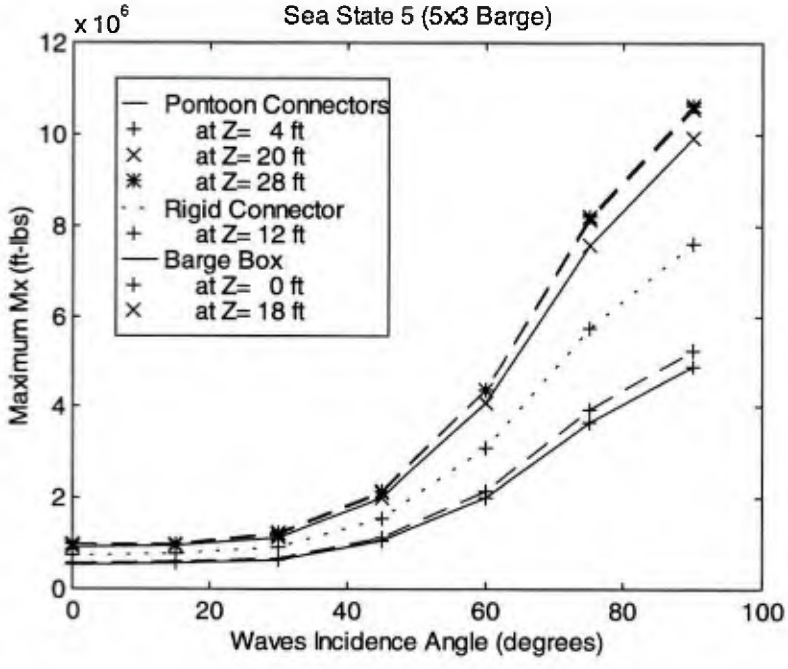

Figure 2.74 Comparison of M_x

3.0 CONCLUSIONS AND RECOMMENDATIONS

Considering all wave directions and free body cuts at different cross sections, the maximum shear force F_y and bending moments M_x and M_z are tabulated in Tables 3.1 through 3.8 for each platform size and displayed in Figures 3.1 through 3.8. These figures are shown in a 3-dimensional format with the X-axis showing the number of longitudinal modules, the Y-axis showing the number of transverse modules, and the Z-axis showing the maximum connector/section loads, F_y, M_x, or M_z. Based on the parametric study conducted, conclusions and recommendations are drawn and presented below.

(1) This parametric study has focused on the analysis of connector loads. However, the motion responses of the platform are computed and available. In some cases, the pitch and roll response exceeds approximately 17 degrees in the survival sea state.

(2) If the motion response is of interest in the future, additional analyses should be performed assuming the platform is partially loaded rather than using the assumption of a fully loaded condition as was used in this study. Additionally, the mass distribution should be placed on the platform as close to the real condition as possible rather than using the assumption of uniform distribution on the surface of the box-like shell structure.

(3) The most critical force component is the vertical shear F_y and the most critical bending moment is either M_x and M_z depending on the imaginary cuts along the X-axis or Z-axis.

(4) For all of the cases studied herein, the most critical section in terms of maximum force component, F_y, is not located at X = 0 ft or Z = 0 ft. Instead, the critical section is located near the end of the platform because the large pitch or roll motion probably induced a significant amount of pressure force in the Y-direction of the body coordinate.

(5) For all of cases studied, the most critical section, in terms of the maximum bending moment M_z, is located at X = 0 ft. The most critical section, in terms of maximum bending moment M_x, is not necessarily located at Z = 0 ft, which is consistent with Conclusion (4) given above.

(6) From all the analyses on free bodies by transverse cuts at X=constant ft, the widest platform has the most critical force component F_y for those with the same length. For platforms with same width, the longest platform has the most critical force component F_y . This conclusion simply follows common sense. However, from all the analyses on free bodies by longitudinal cuts at Z=constant ft, the widest platform does not necessarily have the most critical force component F_y for those with the same length (see Figures 3.5 and 3.6). The longest platform still has the most critical force component F_y for those with the same width.

(7) For platforms with same length, the widest platform has the most critical bending moment components M_x and M_z . For platforms with the same width, the longest platform exhibits the most critical bending moment components M_x and M_z . Once again, this reasoning is straight forward.

(8) The maximum bending moment component M_z occurs at X = 0 ft in head seas (0 degrees) while the maximum bending moment component M_x occurs at Z = 0 ft in beam seas (90 degrees).

(9) Data collected in the planned Logistics Engineering Advanced Demonstration (LEAD) for an Advanced Lighterage for High Sea States Operation should be used to verify this simulation's results.

Table 3.1 Maximum Shear Force, F_y, for Sea State 3
(Transverse Cuts at X=Constant)

	LENGTH			
WIDTH	2 Modules	3 Modules	4 Modules	5 Modules
1 Module	.4666E+04 lbs	.3222E+05 lbs	.4862E+05 lbs	.6221E+05 lbs
2 Modules	.7228E+04 lbs	.5587E+05 lbs	.8037E+05 lbs	.9469E+05 lbs
3 Modules	.1045E+05 lbs	.8089E+05 lbs	.1132E+06 lbs	.1227E+06 lbs

Table 3.2 Maximum Shear Force, F_y, for Sea State 5
(Transverse Cuts at X=Constant)

	LENGTH			
WIDTH	2 Modules	3 Modules	4 Modules	5 Modules
1 Module	.6274E+04 lbs	.6222E+05 lbs	.1220E+06 lbs	.1750E+06 lbs
2 Modules	.9672E+04 lbs	.1111E+06 lbs	.2113E+06 lbs	.2977E+06 lbs
3 Modules	.1412E+05 lbs	.1603E+06 lbs	.2976E+06 lbs	.4121E+06 lbs

Table 3.3 Maximum Bending Moment, M_z, for Sea State 3
(Transverse Cuts at X=Constant)

	LENGTH			
WIDTH	2 Modules	3 Modules	4 Modules	5 Modules
1 Module	.7883E+06 ft-lbs	.1667E+07 ft-lbs	.2780E+07 ft-lbs	.4229E+07 ft-lbs
2 Modules	.1526E+07 ft-lbs	.3045E+07 ft-lbs	.4848E+07 ft-lbs	.6822E+07 ft-lbs
3 Modules	.2281E+07 ft-lbs	.4479E+07 ft-lbs	.7050E+07 ft-lbs	.9670E+07 ft-lbs

Table 3.4 Maximum Bending Moment, M_z, for Sea State 5
(Transverse Cuts at X=Constant)

	LENGTH			
WIDTH	2 Modules	3 Modules	4 Modules	5 Modules
1 Module	.1128E+07 ft-lbs	.3113E+07 ft-lbs	.6574E+07 ft-lbs	.1165E+08 ft-lbs
2 Modules	.2190E+07 ft-lbs	.5739E+07 ft-lbs	.1164E+08 ft-lbs	.2010E+08 ft-lbs
3 Modules	.3269E+07 ft-lbs	.8375E+07 ft-lbs	.1664E+08 ft-lbs	.2820E+08 ft-lbs

Table 3.5 Maximum Shear Force, F_y, for Sea State 3
(Longitudinal Cuts at Z=Constant)

	LENGTH			
WIDTH	2 Modules	3 Modules	4 Modules	5 Modules
1 Module	.5585E+05 lbs	.8235E+05 lbs	.1091E+06 lbs	.1359E+06 lbs
2 Modules	.2772E+05 lbs	.4178E+05 lbs	.5589E+05 lbs	.7002E+05 lbs
3 Modules	.4338E+05 lbs	.6435E+05 lbs	.8566E+05 lbs	.1068E+06 lbs

Table 3.6 Maximum Shear Force, F_y, for Sea State 5
(Longitudinal Cuts at Z=Constant)

	LENGTH			
WIDTH	2 Modules	3 Modules	4 Modules	5 Modules
1 Module	.7245E+05 lbs	.1072E+06 lbs	.1422E+06 lbs	.1773E+06 lbs
2 Modules	.4488E+05 lbs	.6810E+05 lbs	.9135E+05 lbs	.1146E+06 lbs
3 Modules	.8415E+05 lbs	.1263E+06 lbs	.1689E+06 lbs	.2113E+06 lbs

Table 3.7 Maximum Bending Moment, M_x, for Sea State 3
(Longitudinal Cuts at Z=Constant)

	LENGTH			
WIDTH	2 Modules	3 Modules	4 Modules	5 Modules
1 Module	.2929E+06 ft-lbs	.4325E+06 ft-lbs	.5736E+06 ft-lbs	.7137E+06 ft-lbs
2 Modules	.8114E+06 ft-lbs	.1216E+07 ft-lbs	.1621E+07 ft-lbs	.2028E+07 ft-lbs
3 Modules	.2371E+07 ft-lbs	.3514E+07 ft-lbs	.4679E+07 ft-lbs	.5836E+07 ft-lbs

Table 3.8 Maximum Bending Moment, M_x, for Sea State 5
(Longitudinal Cuts at Z=Constant)

	LENGTH			
WIDTH	2 Modules	3 Modules	4 Modules	5 Modules
1 Module	.3559E+06 ft-lbs	.5267E+06 ft-lbs	.6994E+06 ft-lbs	.8705E+06 ft-lbs
2 Modules	.1279E+07 ft-lbs	.1932E+07 ft-lbs	.2586E+07 ft-lbs	.3240E+07 ft-lbs
3 Modules	.4507E+07 ft-lbs	.6762E+07 ft-lbs	.9039E+07 ft-lbs	.1131E+08 ft-lbs

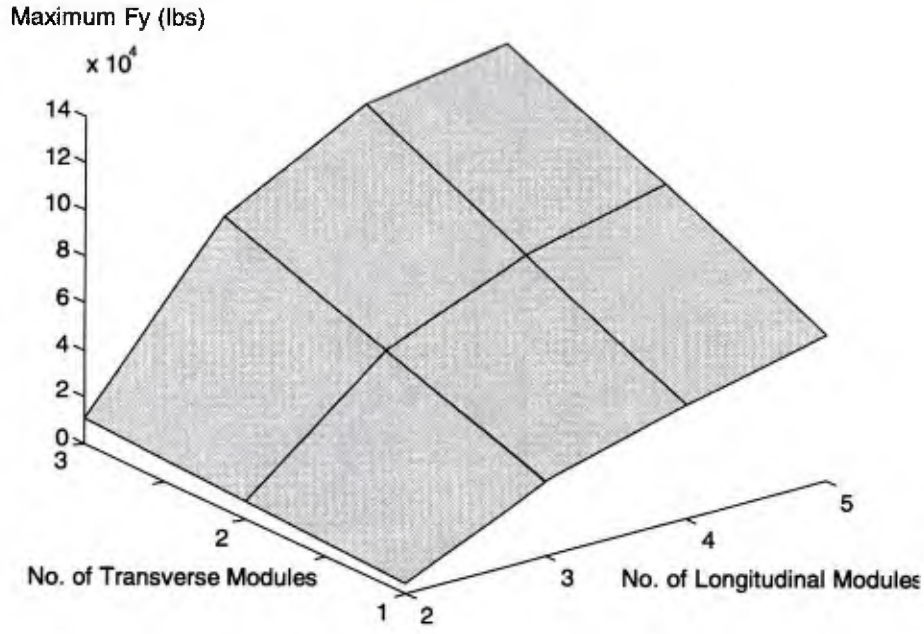

Figure 3.1 Maximum Shear Force, F_y, for Sea State 3
(Transverse Cuts at X=Constant)

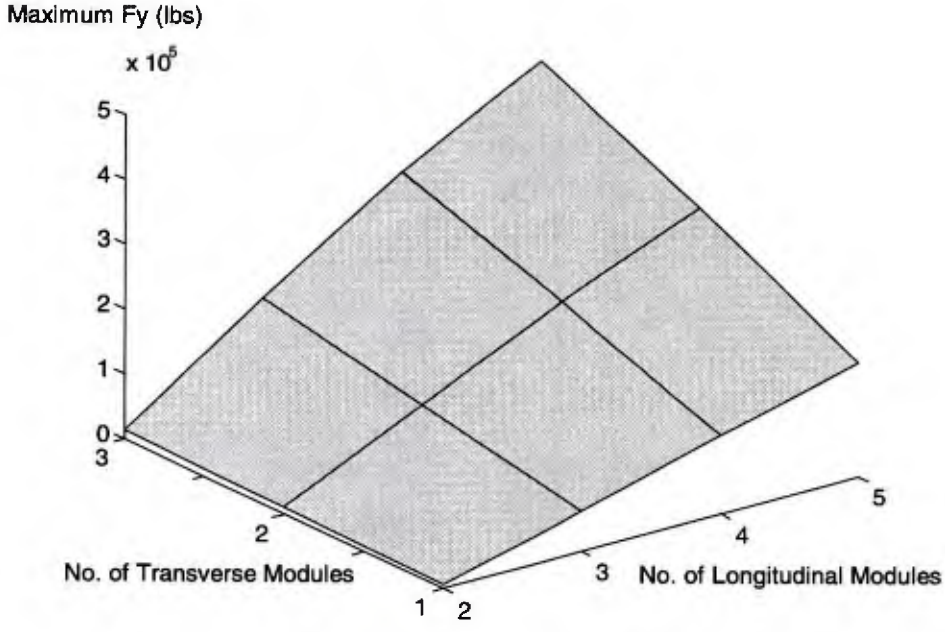

Figure 3.2 Maximum Shear Force, F_y, for Sea State 5
(Transverse Cuts at X=Constant)

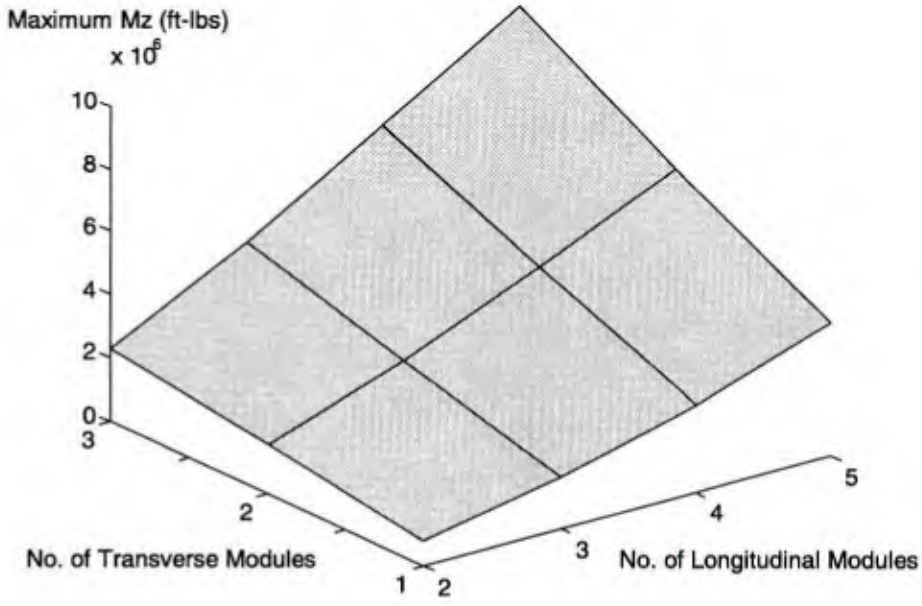

Figure 3.3 Maximum Bending Moment, M_z, for Sea State 3
(Transverse Cuts at X=Constant)

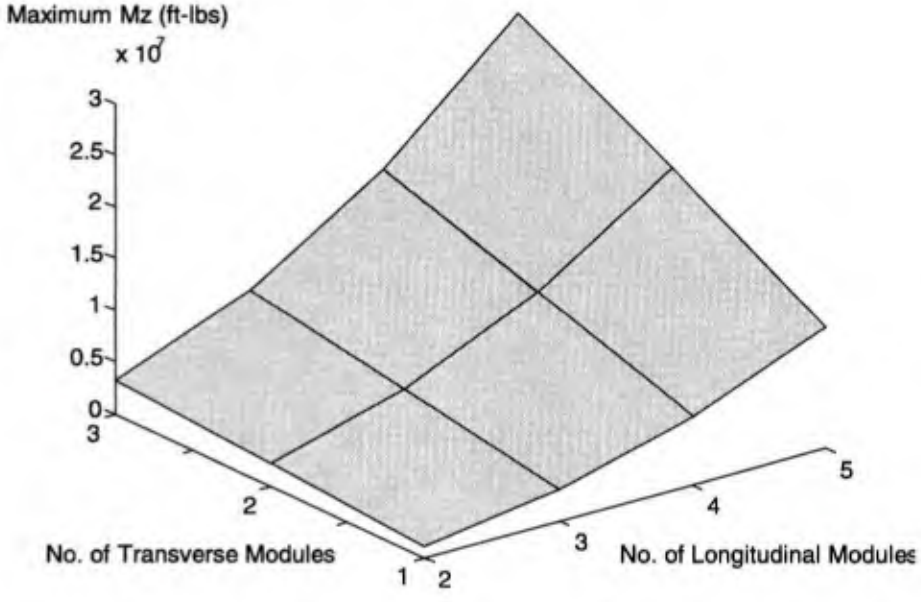

Figure 3.4 Maximum Bending Moment, M_z, for Sea State 5
(Transverse Cuts at X=Constant)

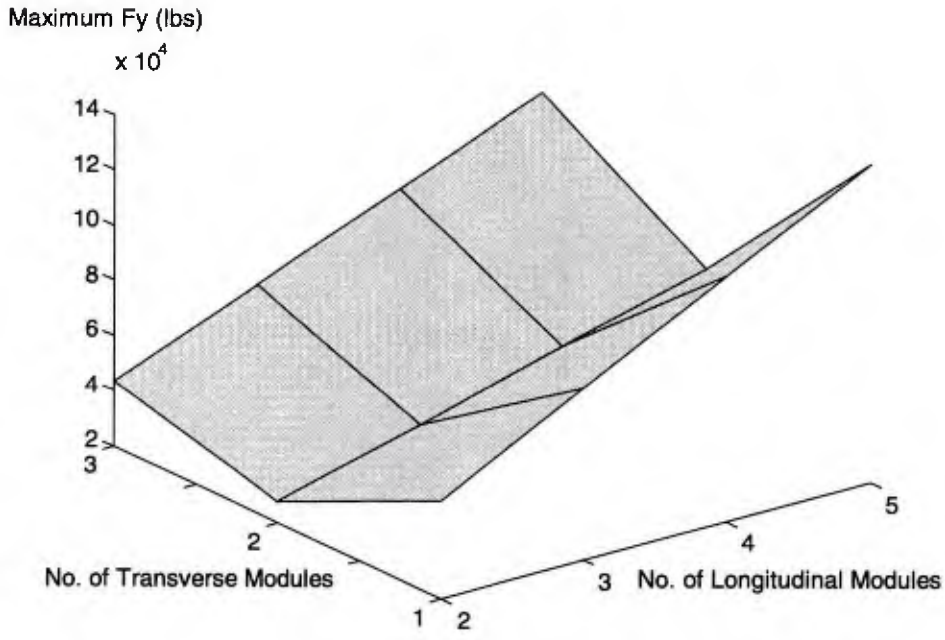

Figure 3.5 Maximum Shear Force, F_y, for Sea State 3
(Longitudinal Cuts at Z=Constant)

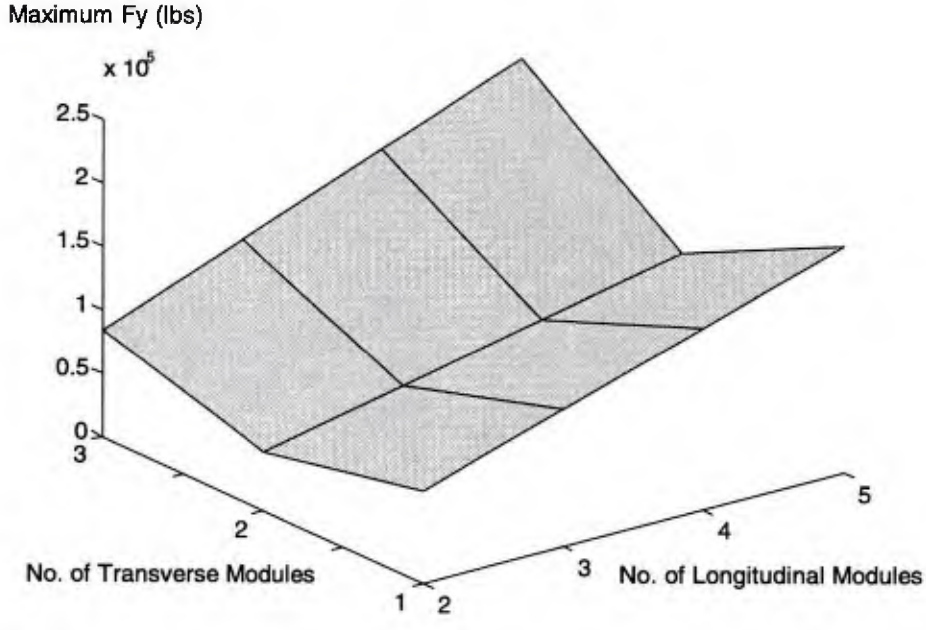

Figure 3.6 Maximum Shear Force, F_y, for Sea State 5
(Longitudinal Cuts at Z=Constant)

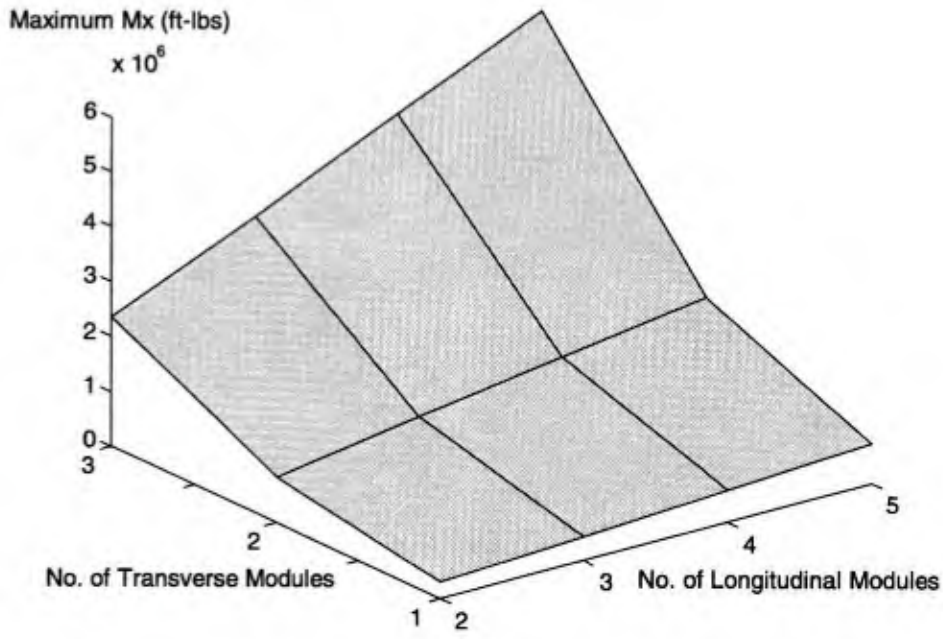

Figure 3.7 Maximum Bending Moment, M_x, for Sea State 3
(Longitudinal Cuts at Z=Constant)

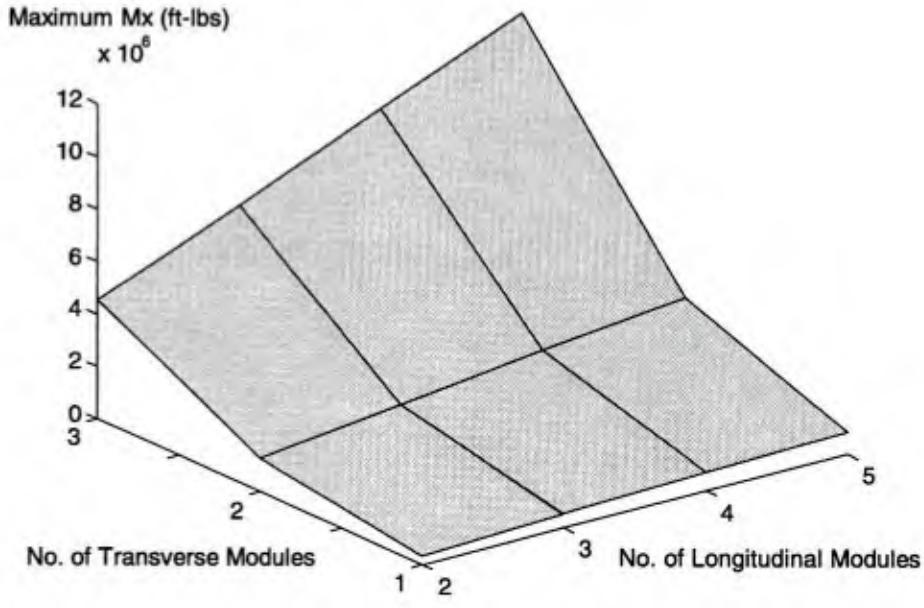

Figure 3.8 Maximum Bending Moment, M_x, for Sea State 5
(Longitudinal Cuts at Z=Constant)

REFERENCE:

1. Garrison, C.J, 1995, MORA USER'S GUIDE, C.J. Garrison & Associates, Corvallis, Oregon 97333